

1 **Intra-annual variability of the Western Mediterranean Oscillation (WeMO)**
2 **and occurrence of extreme torrential precipitation in Catalonia (NE Iberia)**

3 J.A. Lopez-Bustins (1), L. Arbiol-Roca (1), J. Martin-Vide (1), A. Barrera-Escoda
4 (2) and M. Prohom (1, 2)

5 (1) Climatology Group, Department of Geography, University of Barcelona
6 (UB), Barcelona, Spain.

7 (2) Department of Climatology, Meteorological Service of Catalonia,
8 Barcelona, Spain.

9
10 **Abstract**

11 In previous studies the Western Mediterranean Oscillation index (WeMOi) at daily
12 resolution has proven to constitute an effective tool for analysing the occurrence of
13 episodes of torrential precipitation over eastern Spain. The Western Mediterranean
14 region is therefore a very sensitive area, since climate change can enhance these
15 weather extremes. In the present study we created a catalogue of the extreme
16 torrential episodes (≥ 200 mm in 24 hours) that took place in Catalonia (NE Iberia)
17 during the 1951-2016 study period (66 years). We computed daily WeMOi values
18 and constructed WeMOi calendars. Our principal results reveal the occurrence of
19 50 episodes (0.8 cases per year), mainly concentrated in the autumn. We
20 confirmed a threshold of WeMOi ≤ -2 to define an extreme negative WeMO phase
21 at daily resolution. Most of the 50 episodes (60%) in the study area occurred on
22 days presenting an extreme negative WeMOi value. Specifically, the most negative
23 WeMOi values are detected in autumn, during the second 10-day period of October
24 (11th-20th), coinciding with the highest frequency of extreme torrential events. On
25 comparing the subperiods, we observed a statistically significant decrease in
26 WeMOi values in all months, particularly in late October, and in November and
27 December. No changes in the frequency of these extreme torrential episodes were
28 observed between both subperiods. In contrast, a displacement of the extreme
29 torrential episodes is detected from early to late autumn; this can be related to a
30 statistically significant warming of sea temperature.

31 **Keywords**

32 Mediterranean, sea temperature, teleconnection indices, torrential precipitation,
33 WeMO.

34 1. Introduction

35 The Mediterranean seasonal precipitation regime is characterised by rainy
36 winters and dry summers, linked to the westerly atmospheric circulation in winter
37 and to the subtropical anticyclone belt in summer. Nevertheless, in some regions
38 of the Mediterranean basin, the seasonal precipitation regime differs from the
39 typically Mediterranean one; for example, most of eastern Iberia (Spain) displays
40 a seasonal precipitation maximum in autumn, and a secondary one in spring (De
41 Luis *et al.*, 2010; González-Hidalgo *et al.*, 2011). This bimodal precipitation
42 pattern is recorded in few regions of the world. It only occurs over approximately
43 7% of the global land surface, and is commonly associated with locations within
44 the tropics (Knoben *et al.*, 2019). This bimodal behaviour in eastern Spain is
45 mainly due to the physical geographic complexity of the Iberian Peninsula, which
46 comprises several mountain ranges, all of which present different slope
47 orientations. Furthermore, the Mediterranean Sea is practically cut off from other
48 water bodies, which favours a higher sea surface temperature (SST) than in the
49 Atlantic at the same latitude, especially in summer and autumn (Pastor *et al.*,
50 2015). This contributes to the development of high vertical gradients of air
51 temperature in some months over the Mediterranean basin (Estrela *et al.*, 2008;
52 Pérez-Zanón *et al.*, 2018). These physical geographical factors give rise to a high
53 concentration of daily precipitation in the Mediterranean basin, i.e. torrential
54 precipitation events, above all in the Western Mediterranean (Beguería *et al.*,
55 2011; Cortesi *et al.*, 2012; Caloiero *et al.*, 2019); all this reveals the need for water
56 management in Spain to be based upon precipitation variability rather than on
57 the precipitation mean (Lopez-Bustins, 2018). Heavy precipitation in the Western
58 Mediterranean is mainly centred in eastern Spain, the south of France and the
59 region of Liguria (NW Italy) (Peñarrocha *et al.*, 2002). These torrential events can
60 cause dangerous floods and can have serious social and economic
61 consequences, even human casualties, in the Mediterranean regions, e.g. in
62 eastern Spain (Olcina *et al.*, 2016; Kreibich *et al.*, 2017; Nakamura and Llasat,
63 2017; Martin-Vide and Llasat, 2018) and in southern Spain (Gil-Guirado *et al.*,
64 2019; Naranjo-Fernández *et al.*, 2020). Climatological studies on torrential
65 precipitation frequency and intensity are therefore relevant with regard to
66 improving emergency plans and mitigating flood damage. Extreme precipitation

67 is expected to increase with global warming as a result of a greater atmospheric
68 water content (Papalexiou and Montanari, 2019); for instance, extreme peak river
69 flows are predicted to increase in Southern Europe during the current century
70 (Alfieri *et al.*, 2015), and the frequency of heavy precipitation events is projected
71 to be higher for the 2011-2050 period (Barrera-Escoda *et al.*, 2014).

72 Previous studies have associated extreme daily precipitation events in Spain with
73 synoptic patterns (Martin-Vide *et al.*, 2008; Peña *et al.*, 2015); these studies have
74 addressed several different tropospheric levels (Romero *et al.*, 1999; Merino *et al.*
75 *et al.*, 2016; Pérez-Zanón *et al.*, 2018). Furthermore, many studies have also
76 statistically correlated several teleconnection indices (El Niño Southern
77 Oscillation, North Atlantic Oscillation, Arctic Oscillation, Mediterranean
78 Oscillation, Western Mediterranean Oscillation, etc.) with precipitation series for
79 the Iberian Peninsula at different timescales (Rodó *et al.*, 1997; Rodríguez-
80 Puebla *et al.*, 2001; Trigo *et al.*, 2004; Lopez-Bustins *et al.*, 2008; González-
81 Hidalgo *et al.*, 2009; Ríos-Cornejo *et al.*, 2015a; Merino *et al.*, 2016). Among
82 these indices, the Western Mediterranean Oscillation (WeMO) was found to be
83 the index most statistically and significantly correlated with annual, monthly and
84 daily precipitation on the littoral fringe of eastern Spain (Martin-Vide and Lopez-
85 Bustins, 2006; González-Hidalgo *et al.*, 2009). The daily timescale of the WeMO
86 index (WeMOi) could constitute a potential tool for analysing the frequency of
87 torrential events in some regions of the Western Mediterranean basin.

88 Most torrential events in the Mediterranean region present a cyclonic centre at
89 surface level (Jansà *et al.*, 1996; Rigo and Llasat, 2003). These cyclonic centres,
90 which are mainly mesoscale lows, can contribute to the structure of low-level
91 flows and therefore to the creation or intensification of a low-level warm and wet
92 current that can feed and sustain convection in favourable environmental
93 conditions (Jansà and Genovés, 2000; Jansà *et al.*, 2000). Furthermore, the
94 Mediterranean Sea moistens and warms the low level of the atmosphere.
95 Consequently, the southerly to easterly flow that prevails before and during
96 torrential events in the Western Mediterranean transports the air under
97 conditional instability toward the coasts, where convection is often triggered by
98 an interaction between the flow and the orography. Studies based upon
99 mesoscale modelling, such as the research conducted by Lebeaupin *et al.*

100 (2006), show that an increase (or a decrease) in SST by several degrees
101 intensifies (or weakens) convection. In addition, the presence of a cut-off low in
102 the upper troposphere might be playing a significant role in the occurrence of
103 heavy precipitation, creating a cyclonic circulation in the lower troposphere, thus
104 enabling Atlantic air to be carried over the Mediterranean Sea. This warm and
105 very wet air in the lower layers impinges on the coastal mountains ranges and
106 the forced ascent is sufficient to trigger potential instability. This meteorological
107 configuration is accounted for the negative phase of the WeMO, which defines a
108 synoptic pattern prone to producing torrential precipitation and floods on the
109 Eastern Iberian coast. Daily precipitation amounts over 200 mm are not unusual
110 in such cases, particularly in eastern Spain, where many catastrophic floods are
111 related to the presence of a cut-off low (Llasat, 2009). Thus, these catastrophic
112 floods in the Northwestern Mediterranean basin are generally of synoptic origin
113 and are defined by the negative phase of the WeMO and enhanced by certain
114 mesoscale factors (Gilabert and Llasat, 2018).

115 The present study provides an exhaustive inventory of the most intense daily
116 precipitation events in Catalonia (NE Iberia) over the last few decades (1951-
117 2016) in order to provide a better understanding of their temporal distribution.
118 Moreover, we will analyse changes in frequency according to subperiods, since
119 the Western Mediterranean basin constitutes a global warming hotspot, where a
120 decrease in mean annual precipitation is expected for the following decades,
121 particularly in summer, together with a potential rise in storm-related precipitation
122 and drought duration (Christensen *et al.*, 2013; Barrera-Escoda *et al.*, 2014;
123 Cramer *et al.*, 2018; Greve *et al.*, 2018). The main aim of our study involves
124 creating a catalogue of extreme torrential events in Catalonia in order to establish
125 a period of high potential torrentiality in the area analysed at daily resolution. Most
126 studies delimit the wet season of a region within one or several months (Kottek
127 *et al.*, 2006), and do not employ a smaller timescale than the monthly one.
128 Consequently, the present research attempts to use a more accurate timescale
129 than the monthly one in order to determine the period with the highest
130 accumulation of heavy precipitation episodes according to fortnights and 10-day
131 periods. The intra-annual variability of the daily WeMOi values may help to
132 establish the period with the highest propensity for torrential events in Catalonia.

133 Additionally, we analyse SST in order to establish a sea-atmosphere interaction
134 to explain WeMOi values and changes in the frequency of events. Seawater
135 constitutes an energy store, i.e. recharge areas, which can influence water
136 vapour content and can intensify precipitation episodes (Pastor *et al.*, 2018;
137 Iizuka and Nakamura, 2019) by means of a sea-atmosphere moisture exchange.
138 Furthermore, a significant release of latent heat occurs during atmospheric
139 convection over a warm sea like the Mediterranean at the end of summer and the
140 beginning of autumn (Pastor *et al.*, 2015).

141 In section 2, we describe the main orographic and pluviometric features of the study
142 area. The data and methods followed to calculate daily WeMOi values and construct
143 the WeMOi calendar are explained in section 3. In section 4, the results of the intra-
144 annual variability of torrential episodes, WeMOi values and sea temperature trends
145 are analysed and discussed. Finally, in section 4 we derive the conclusions.

146

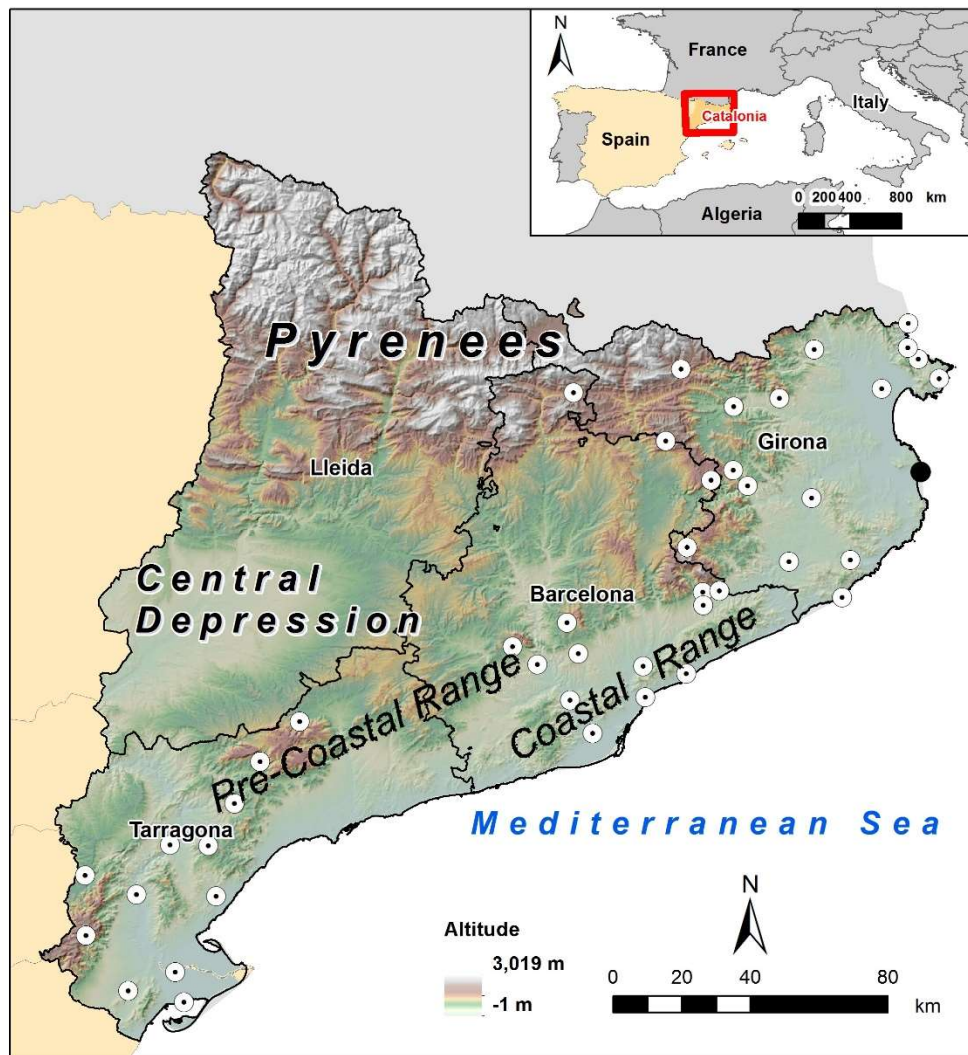
147 **2. Study area**

148 Catalonia covers an area of 32,100 km² in northeast Spain; it is physically separated
149 from France by the Pyrenees (Figure 1). Altitude ranges from 0 (littoral) to 3,100
150 (northwestern Pyrenees) m.a.s.l. The Coastal and Pre-Coastal ranges, with an
151 altitude ranging from 500 to 1,700 m.a.s.l., present a SW-NE orientation. On the
152 western border, the Central Depression is approximately 200-300 m.a.s.l.,
153 constituting the driest part of the study area (350 mm annual mean precipitation)
154 (Figure 2a). The wettest part of Catalonia is located in the Pyrenees, with an annual
155 mean precipitation over 1,200 mm. In general terms, southern Lleida and Barcelona,
156 as well as almost the entire province of Tarragona, make up the dry part of Catalonia
157 (<700 mm). The rainy part of Catalonia (≥ 700 mm) comprises the province of Girona
158 and the northern halves of the provinces of Lleida and Barcelona.

159 Catalonia's complex orography, as well as the fact that it comes under the influence
160 of the Atlantic Ocean and the Mediterranean Sea, endow it with a highly
161 heterogeneous spatial distribution of seasonal precipitation regimes throughout the
162 study area. Using 70 monthly precipitation series (1951-2016) homogenized and
163 provided by the Meteorological Service of Catalonia (SMC, 2017), we ascertained
164 that, of the total of 24 possible permutations between winter, spring, summer and

165 autumn as dominant and subdominant precipitation seasons, 7 of these are detected
166 in Catalonia (Figure 2b) (Martin-Vide and Raso-Nadal, 2008). A clear predominance
167 of autumn precipitation can be observed, followed by spring precipitation, especially
168 in the coastal zone. The driest season on the coast is summer; however, the driest
169 time of year inland is winter. Many areas of the Pyrenees, above all in the east,
170 exhibit their maxima in summer as a result of convective precipitation.

171

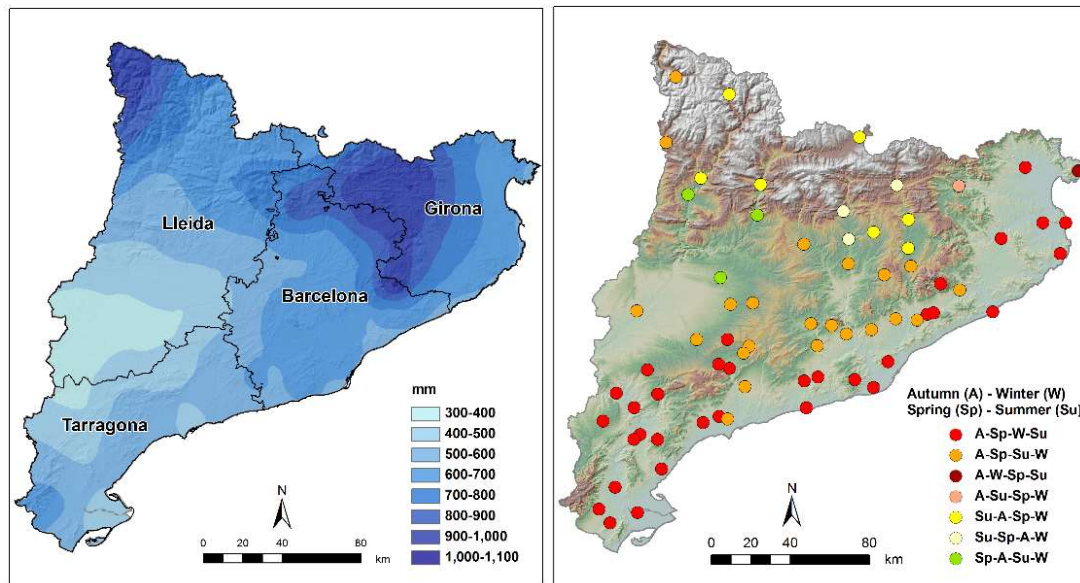


172

173 Figure 1. Location of Catalonia (NE Spain) within Europe, altitude and provinces.
174 The white dots indicate the 43 different weather stations that have recorded the
175 highest precipitation amount during an extreme torrential event at least once in
176 Catalonia during the 1951-2016 study period. The black dot indicates the location
177 of the sea temperature series. Base map provided by the Cartographic and
178 Geological Institute of Catalonia.

(a)

(b)



180

181 Figure 2. (a) Annual mean precipitation (mm) and (b) seasonal precipitation
 182 regimes for 70 weather stations in Catalonia for the 1951-2016 study period.
 183 Data source: SMC (2017). Base map provided by the Cartographic and
 184 Geological Institute of Catalonia.

185

186 3. Data and methods

187 3.1. Selection of torrential events

188 Several studies have selected the torrential precipitation events in Spain based
 189 on the threshold of 100 mm in 24 h (Pérez-Cueva, 1994; Martin-Vide and Llasat,
 190 2000; Armengot, 2002; Riesco and Alcover, 2003; Martin-Vide *et al.*, 2008).
 191 Herein we chose the extreme torrential episodes (≥ 200 mm in 24 h) (Martin-Vide,
 192 2002; Lopez-Bustins *et al.*, 2016) that took place over Catalonia during the 1951-
 193 2016 study period (66 years). We consider the threshold of 200 mm in 24 h to
 194 present a natural risk in most cases, with significant consequences. Episodes
 195 involving ≥ 100 mm in 24 h are more frequent, but sometimes have no direct
 196 impact, or quite a negligible effect, because other factors are the main drivers of
 197 floods, e.g. precipitation duration (Jang, 2015), initial soil moisture conditions and
 198 hydrological parameters (Norbiato *et al.*, 2008; Martina *et al.*, 2009). Furthermore,
 199 the area affected by episodes of ≥ 100 mm in 24 h is sometimes local and is

200 therefore not easily associated with advective synoptic patterns (Gilabert and
201 Llasat, 2018).

202 In order to select the extreme torrential events, we considered all available
203 precipitation data sources in Catalonia (Meteorological Service of Catalonia,
204 Spanish National Meteorological Agency, Catalan Water Agency and Ebro
205 Hydrographic Confederation). Thus, 1,466 weather stations were identified
206 during 1951-2016, of which 986 were manually managed (67.3%) and provided
207 one register per day, at 7 h UTC. Until 1987 the manual weather stations had
208 constituted the only precipitation data source in Catalonia. The remaining 480
209 weather stations were automatic observatories, reporting hourly or semi-hourly
210 data depending on the network and period. The 1988-2016 period was covered
211 by both manual and automatic stations. We considered the pluviometric day as
212 7-7 UTC in both types of observatories in order to ensure a homogeneous
213 criterion when selecting episodes along the whole study period and analysing any
214 temporal changes in their frequency. We conducted an exhaustive spatial and
215 temporal verification of the extreme torrential episodes identified. We tested the
216 reliability of the events considering the daily precipitation recorded in
217 neighbouring stations and examining the original handwritten observation cards.
218 Furthermore, we rectified several episodes recorded by weather stations the day
219 after the pluviometric day, and we eliminated events derived from the
220 accumulation of precipitation for over one day.

221 The catalogue of extreme torrential events in Catalonia contains the following
222 columns: date, maximum precipitation in 24 h, location, province and daily
223 WeMOi value. Several observatories in Catalonia can occasionally register ≥ 200
224 mm in 24 h on one same date, but only the highest amount was taken into
225 account. Finally, we obtained 50 extreme torrential events for consideration in the
226 present study (Table 1). A total of 32 out of the 50 episodes (64%) have a decimal
227 place of 0, and 10 out of the 50 episodes (20%) present a decimal place of 5.
228 Most of these episodes were registered by manual weather stations prior to the
229 1990s. This is known as the rounding effect (Wergen *et al.*, 2012): a weather
230 observer rounds off the daily precipitation accumulation value during heavy
231 precipitation events. This effect has no influence on the results of the present
232 research.

Date	Max RR (mm)	Location	Province	WeMOi value
13 October 1986	430.0	Cadaqués	Girona	-2.22
11 April 2002	367.5	Darnius	Girona	-3.85
20 September 1971	308.0	Esparreguera	Barcelona	-1.75
20 September 1972	307.0	Sant Carles de la Ràpita	Tarragona	-1.58
09 October 1994	293.0	Cornudella de Montsant	Tarragona	-2.88
03 October 1987	291.0	Castelló d'Empúries	Girona	-1.96
22 September 1971	285.0	Cadaqués	Girona	-2.19
19 October 1977	276.0	Cadaqués	Girona	-2.80
21 September 1971	275.0	Santa Maria de Palautordera	Barcelona	-2.21
18 October 1977	271.8	Camprodon	Girona	-2.21
21 October 2000	270.0	Falset	Tarragona	-2.26
07 November 1982	266.0	la Pobla de Lillet	Barcelona	-5.56
12 October 2016	257.0	Vilassar de Mar	Barcelona	-1.86
05 March 2013	253.5	Darnius	Girona	-5.32
29 November 2014	253.5	Parc Natural dels Ports	Tarragona	-4.54
16 February 1982	251.2	Amer	Girona	-2.41
25 September 1962	250.0	Martorelles	Barcelona	-1.52
04 November 1962	248.5	Sant Llorenç del Munt	Barcelona	-2.79
<i>02 September 1959</i>	<i>246.5</i>	<i>Cadaqués</i>	<i>Girona</i>	<i>-0.84</i>
10 October 1994	245.0	Beuda	Girona	-2.33
22 October 2000	240.0	Tivissa	Tarragona	-2.50
12 November 1999	233.5	Castellfollit de la Roca	Girona	-3.00
06 January 1977	233.0	Girona	Girona	-2.22
20 December 2007	230.2	Parc Natural dels Ports	Tarragona	-3.54
06 October 1959	230.1	Tossa de Mar	Girona	-1.36
03 October 1951	230.0	Cornellà de Llobregat	Barcelona	-1.02
20 September 1959	230.0	Gualba de Dalt	Barcelona	-1.49
11 October 1970	230.0	Riudabella	Tarragona	-1.61
23 October 2000	229.0	Horta de Sant Joan	Tarragona	-2.41
26 September 1992	226.4	Ampostà	Tarragona	-2.22
04 April 1969	226.0	Rupit	Barcelona	-2.21
12 November 1988	225.0	Corbera de Llobregat	Barcelona	-2.76
11 October 1962	223.0	Sils	Girona	-1.20
<i>20 November 1956</i>	<i>221.0</i>	<i>Cornellà de Llobregat</i>	<i>Barcelona</i>	<i>-0.45</i>
06 November 1983	220.0	Terrassa	Barcelona	-2.34
19 October 1994	220.0	el Port de Llançà	Girona	-2.36
<i>31 July 2002</i>	<i>218.2</i>	<i>Badalona</i>	<i>Barcelona</i>	<i>-0.13</i>
13 September 1963	217.5	l'Ametlla de Mar	Tarragona	-1.14
<i>19 September 1971</i>	<i>217.0</i>	<i>Xerta</i>	<i>Tarragona</i>	<i>-0.97</i>
<i>17 September 2010</i>	<i>216.8</i>	<i>l'Ametlla de Mar</i>	<i>Tarragona</i>	<i>-0.60</i>
17 October 2003	213.0	Vidrà	Girona	-2.48
<i>09 June 2000</i>	<i>210.0</i>	<i>el Bruc</i>	<i>Barcelona</i>	<i>-0.23</i>
<i>31 August 1975</i>	<i>208.5</i>	<i>Santa Agnès de Solius</i>	<i>Girona</i>	<i>-0.15</i>
29 January 1996	206.5	Fogars de Montclús	Barcelona	-2.37
<i>09 October 1971</i>	<i>204.0</i>	<i>Miravet</i>	<i>Tarragona</i>	<i>-0.86</i>
26 December 2008	202.5	Darnius	Girona	-2.84
07 May 2002	200.8	Godall	Tarragona	-2.47
07 October 1965	200.0	les Planes d'Hostoles	Girona	-2.12
27 October 1989	200.0	el Port de la Selva	Girona	-1.90
01 November 1993	200.0	Portbou	Girona	-2.57

233 Table 1. Catalogue of extreme torrential events (≥ 200 mm in 24 h, 7-7 UTC) in
234 Catalonia (NE Iberia) during the 1951-2016 period. Max RR is the highest
235 precipitation accumulation of the episode. The events are classified according to
236 the extreme negative Western Mediterranean Oscillation (WeMO) phase (bold),
237 the negative WeMO phase and the slight negative WeMO phase (italics).

238 3.2. Daily WeMOi values

239 The WeMOi is a regional teleconnection index defined within the Western
240 Mediterranean basin (Martin-Vide and Lopez-Bustins, 2006) and already used in
241 a wider range of studies (Azorin-Molina and Lopez-Bustins, 2008; Vicente-
242 Serrano *et al.*, 2009; Caloiero *et al.*, 2011; El Kenawy *et al.*, 2012; Coll *et al.*,
243 2014; Ríos-Cornejo *et al.*, 2015b; Lana *et al.*, 2017; Jghab *et al.*, 2019). WeMOi
244 values are computed by means of surface pressure data from the San Fernando
245 (SW Spain) and Padua (NE Italy) weather stations (Figure 3); the synoptic
246 window 30°-60°N - 15°W-20°E is found to best represent WeMO phases (Arbiol-
247 Roca *et al.*, 2018). Pressure data for both series were extracted from Martin-Vide
248 and Lopez-Bustins (2006), who performed a statistical treatment of
249 homogenization and the Climatology Group (University of Barcelona) periodically
250 update the data. The positive phase of the WeMO corresponds to the anticyclone
251 over the Azores encompassing the southwest quadrant of the Iberian Peninsula
252 and low pressures in the Gulf of Genoa (Figure 3a); its negative phase coincides
253 with an anticyclone located over Central or Eastern Europe and a low-pressure
254 centre, often cut off from the northern latitudes, within the framework of the
255 Iberian southwest (Figure 3b). Martin-Vide and Lopez-Bustins (2006) found that
256 the WeMOi was significantly and statistically correlated with precipitation over
257 areas that were weakly influenced by the North Atlantic Oscillation (NAO): these
258 areas are the northernmost and easternmost parts of Spain; precipitation over
259 the Cantabrian fringe (northern Spain) is strongly and positively correlated with
260 the WeMOi, and precipitation over the Spain's eastern façade is strongly and
261 negatively correlated with the WeMOi.

262

263

264

265

266

267

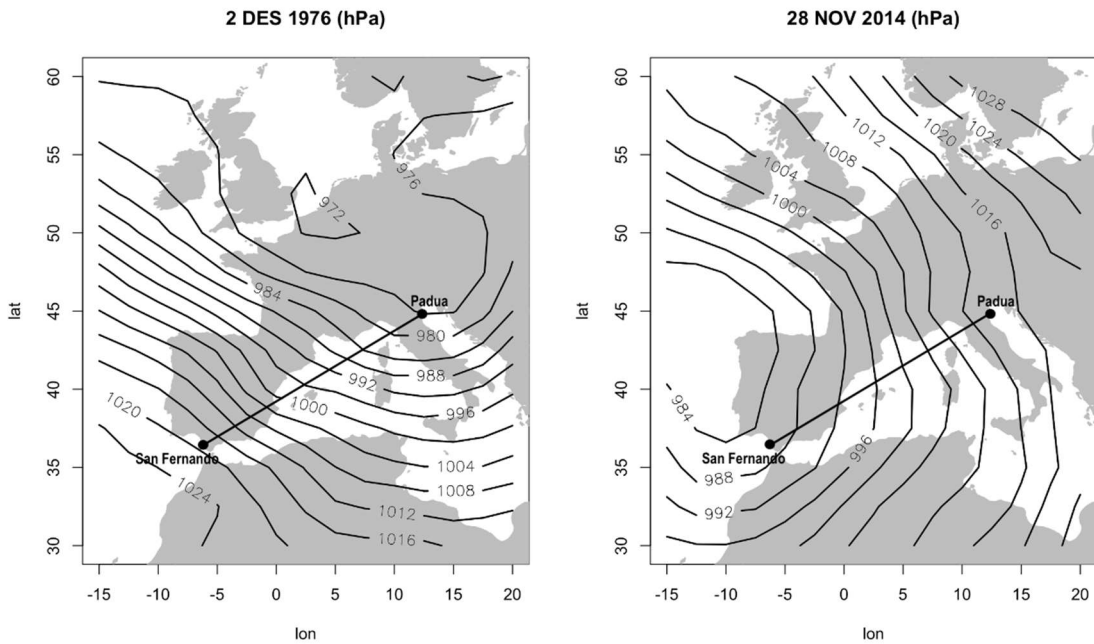
268

269

270

(a)

(b)



272

273 Figure 3. (a) Most extreme positive phase of the Western Mediterranean Oscillation
 274 (WeMO) in a daily synoptic situation during the 1951-2016 study period (2nd
 275 December 1976). (b) Most extreme negative WeMO phase in a daily synoptic situation
 276 during the 1951-2016 study period (28th November 2014). Data source: NCEP
 277 Reanalysis data provided by the NOAA/OAR/ESRL PSD, Boulder, Colorado, USA.

278 Application of the daily WeMOi is a methodological contribution by Martin-Vide
 279 and Lopez-Bustins (2006). It converts the low-frequency feature of the
 280 teleconnection patterns into a high-frequency mode. It is suitable for application
 281 both to the regional scale of the WeMO teleconnection pattern and the lesser
 282 variability of atmospheric pressure at Mediterranean latitudes. Patterns have
 283 rarely been used at daily resolution (Baldwin and Dunkerton, 2001; Beniston and
 284 Jungo, 2002; Azorin-Molina and Lopez-Bustins, 2008; Liu *et al.*, 2018). The
 285 method selected consists of previously standardizing each series of the dipole. It
 286 is necessary to use the daily mean and standard deviation of the 1961-1990
 287 reference period of all days of the year (January 1st 1961 – December 31st 1990).

288

289 For example, the WeMOi on January 1st 1981

290

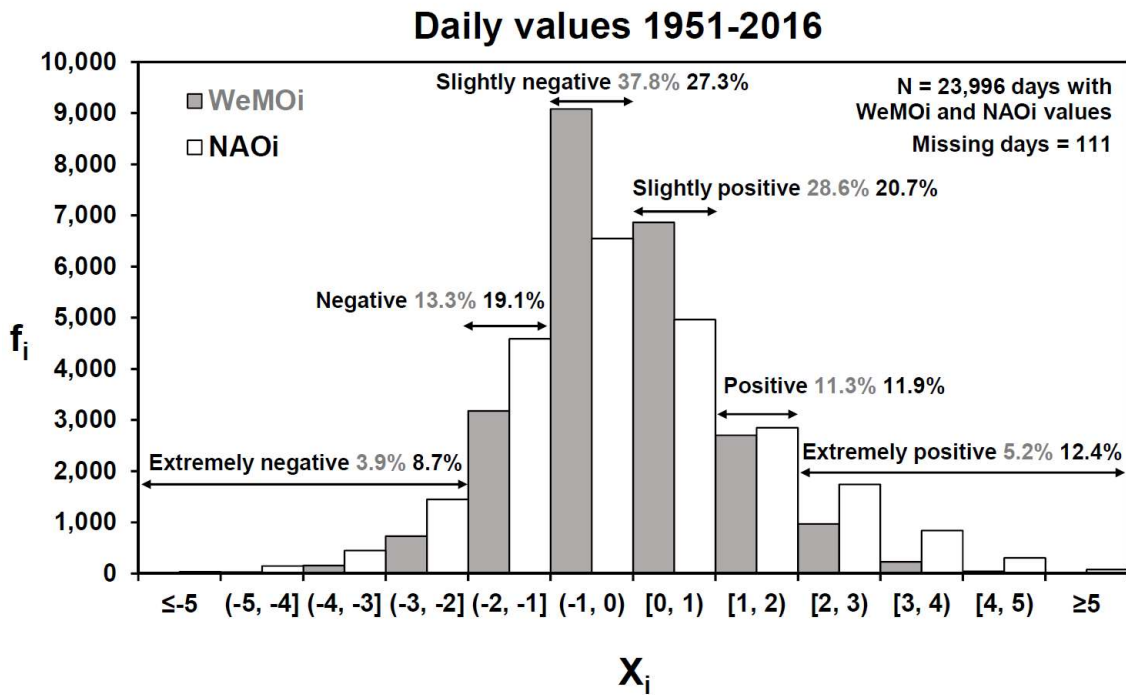
291
$$Z \text{ WeMOi Jan 1st 1981} = \frac{P \text{ Jan 1st 1981 SF} - \bar{X} \text{ 1961}_{1990} \text{ SF}}{S \text{ 1961}_{1990} \text{ SF}} - \frac{P \text{ Jan 1st 1981 PD} - \bar{X} \text{ 1961}_{1990} \text{ PD}}{S \text{ 1961}_{1990} \text{ PD}},$$

292 where P is pressure, SF, San Fernando, PD, Padua, \bar{X} , mean, and S, standard
293 deviation.

294

295 This calculation method, which considers all days of the year in the reference
296 period, enables all Mediterranean flows (negative WeMO phase) to be detected,
297 even if they are very weak. Otherwise, these moderate Mediterranean winds
298 would not be detected in autumn, since the WeMOi means are clearly negative
299 during this season. Likewise, the weak Mediterranean flows would be
300 overestimated in winter due to the high WeMOi mean during the coldest months.
301 According to previous studies (Martin-Vide and Lopez-Bustins, 2006; Azorin-
302 Molina and Lopez-Bustins, 2008), in the histogram of daily WeMOi frequencies,
303 WeMOi values between -1.00 and 1.00 are considered to constitute a neutral
304 WeMO phase, values ranging from 1.00 to 1.99 are considered as a positive
305 WeMO phase, those between -1.99 and -1.00 as a negative WeMO phase,
306 values ≥ 2.00 are deemed to represent an extreme positive WeMO phase and
307 those ≤ -2.00 to indicate an extreme negative WeMO phase. The most positive
308 WeMOi value (+5.99) of the 1951-2016 study period refers to December 2nd
309 1976 (Figure 3a), when an intense precipitation episode was recorded in the
310 Basque Country (northern Spain), according to ECA dataset (Klein Tank *et al.*,
311 2002; Cornes *et al.*, 2018). The most negative WeMOi value (-5.97) during the
312 1951-2016 period corresponds to November 28th 2014 (Figure 3b), when 253.5
313 mm was registered in the *Parc Natural dels Ports* (Tarragona) during the following
314 day (Table 1). Lana *et al.* (2016) studied the statistical complexity and
315 predictability of the WeMOi and demonstrated the Gaussian distribution of this
316 index. Most daily WeMOi values are negative (55%) and two thirds of the 23,996
317 days displaying WeMOi values correspond to a neutral WeMO phase (Figure 4).
318 The positive (negative) WeMO phase was detected in 16.5% (17.2%) of the total
319 days presenting a WeMOi value. The extreme WeMOi values, both positive
320 (5.2%) and negative (3.9%), represent less than 10% of the total number of days
321 for which WeMOi values are available. Daily NAO index (NAOi) values are also
322 used for comparison with WeMOi values and to enhance the role played by the
323 WeMO in torrential precipitation. Following the calculation method based on daily
324 WeMOi values, daily NAOi values are computed by means of surface pressure
325 data from the San Fernando (SW Spain) and Reykjavík (SW Iceland) weather

326 stations; the data for Reykjavík were provided by the ECA dataset (Klein Tank *et*
 327 *al.*, 2002). The NAOi values present the same percentage as that of the negative
 328 WeMOi daily values (55.1%) and almost half of the days are around 0. The
 329 distribution of the daily values of the NAOi presents more extreme positive and
 330 negative values than the WeMOi distribution, 12.4 vs 5.2% and 8.7 vs 3.9%,
 331 respectively (Figure 4).



332
 333 Figure 4. Frequency histogram of all daily WeMO index (WeMOi) values and
 334 North Atlantic Oscillation index (NAOi) values during the 1951-2016 study period.

335 3.3. Construction of calendars

336 Construction of calendars is a common procedure in climatological studies (Soler
 337 and Martin-Vide, 2002; Azorin-Molina and Lopez-Bustins, 2008; Meseguer-Ruiz
 338 *et al.*, 2018). They enable the intra-annual variability of the climate variable to be
 339 visualised. We computed daily WeMOi values for the 1951-2016 (66 years) study
 340 period, constructing two WeMOi calendars based upon the mean values obtained
 341 for each month, a 15-day period (i.e. a fortnight) and a 10-day period; the latter
 342 timescale corresponds approximately to the baroclinic prediction period (Holton,
 343 2004). The first climate calendar will show the annual cycle of the WeMOi values
 344 according to months (12 values), the second will display a more detailed intra-
 345 annual oscillation with 24 values and, finally, the 36 WeMOi values derived from
 346 the 10-day calendar will enable the slightest intra-annual variations in the WeMOi

347 to be detected. We will add to these calendars all the extreme torrential events in
348 order to observe correspondences between WeMOi values and heavy
349 precipitation events along the year. In order to detect any changes in the
350 calendars throughout the study period, we consider two subperiods for the
351 construction of two additional calendars: 1951-1983 (33 years) and 1984-2016
352 (33 years). We statistically tested the mean WeMOi values according to
353 subperiods in order to detect statistically significant differences. This statistical
354 significance is computed by means of a Normal distribution test according to
355 several confidence levels: 95.0% ($Z=1.960$), 99.0% ($Z=2.576$) and 99.9%
356 ($Z=3.291$).

357 Additionally, we analysed these calendars according to subperiods, together with
358 changes in SST and subsurface temperature at several depths (20, 50, and 80
359 m.b.s.l.) at a site located on the coast of Girona province (Figure 1). These data
360 constitute a reference series of sea temperature observations for Spain and for
361 the Mediterranean basin due to their long temporal range (almost half a century)
362 and to their availability at several subsurface levels (Salat *et al.*, 2019); the data
363 on the 1973-2017 period were provided by the Meteorological Service of
364 Catalonia. We calculated monthly temporal trends in sea temperatures using the
365 least-square linear fitting, and we estimated the statistical significance by means
366 of the Mann–Kendall non-parametric test (Sneyers, 1992). The standardized
367 values (Z) of sea temperatures were computed at 10-day resolution, and the Z
368 differences were obtained between two 5-yr subperiods from the beginning and
369 the end of the 1973-2017 period: 1973-1977 and 2013-2017; we showed the Z
370 differences for the months of the wet season (September, October and
371 November) for most of Catalonia (Figure 2b), and also for December in order to
372 detect a potential temporal shift of sea warming rates towards the early winter.

373 **4. Results and discussion**

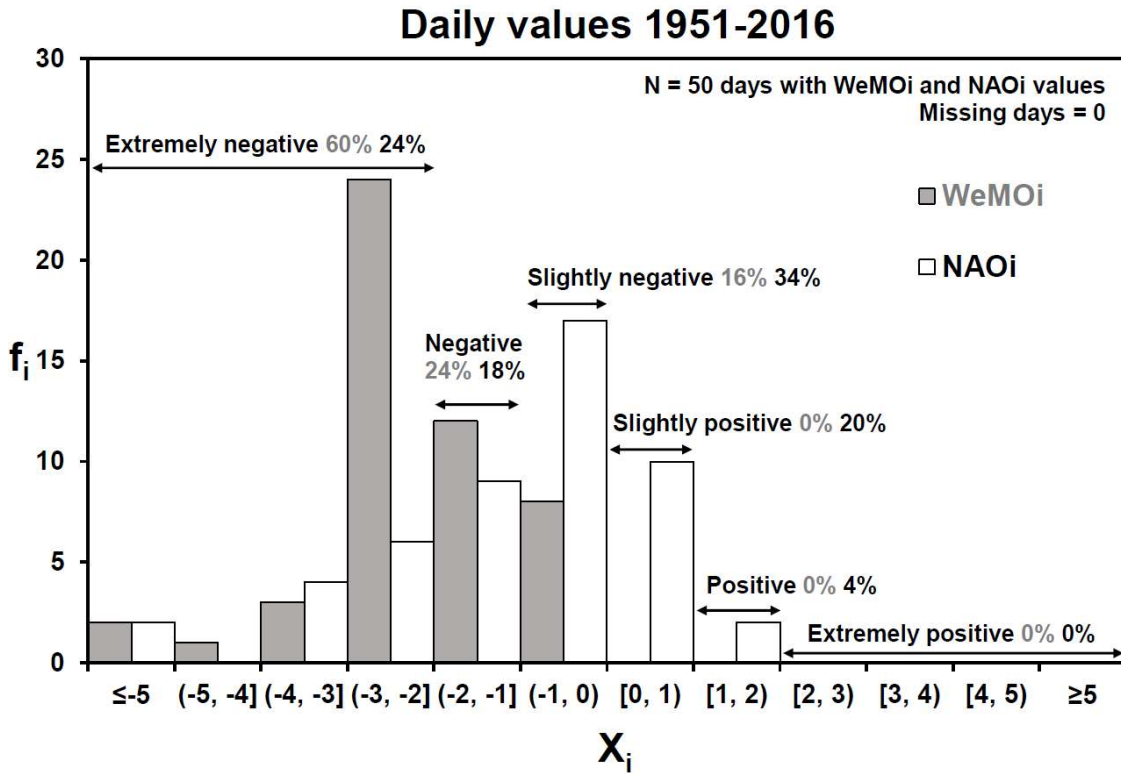
374 *4.1. Frequency and temporal evolution of the extreme torrential events*

375 During the 1951-2016 period, 50 episodes presenting ≥ 200 mm in 24 h were
376 detected (0.8 cases per year) in Catalonia (Table 1); these were mainly
377 concentrated in the Eastern Pyrenees (Girona) and southern Catalonia
378 (Tarragona) (Figure 1), where mountain ranges run in a N-S direction, constituting

379 an orographic barrier to the humid easterly flows (Lopez-Bustins and Lemus-
380 Canovas, 2020). In the province of Lleida no maximum values for precipitation
381 episodes have been recorded, because this province is less influenced by
382 easterly flows as a result of its continental features. Other parts of Iberia register
383 a higher frequency of extreme torrential events, e.g. in the Valencia Region,
384 eastern Spain, there were 2 cases per year during the 1971-2000 period (Riesco
385 and Alcover, 2003). The highest frequency of torrential events (≥ 100 mm in 24 h)
386 over the Iberian Peninsula also corresponds to the Valencia Region, where more
387 than one case per year can be recorded by one same observatory (Pérez-Cueva,
388 1994) and approximately 11 cases per year by all the stations in the Valencia
389 Region (Riesco and Alcover, 2003). Catalonia exhibits a lower frequency of these
390 torrential events (i.e. ≥ 100 mm in 24 h), 5-6 cases per year for the whole region
391 (Martin-Vide and Llasat, 2000; Lopez-Bustins *et al.*, 2016). The highest
392 precipitation amount during 7-7 UTC ever recorded in Catalonia is 430 mm. This
393 occurred in Cadaqués (Cape Creus, in the easternmost part of the Iberian
394 Peninsula) on October 13th 1986. It was an extraordinary episode which also
395 affected the region of Pyrénées-Orientales (S France) (Vigneau, 1987), albeit
396 with a lower amount of precipitation than that produced by other extreme torrential
397 events of over 800 mm in Liguria Region (NW Italy), Valencia Region (E Spain)
398 and this region of Pyrénées-Orientales (Peñarrocha *et al.*, 2002).

399 Most of the episodes in Catalonia (60%) (30 events) took place in an extreme
400 negative (≤ -2.00) WeMO phase (Figure 5), whereas less than 4% of the total
401 number of days with WeMOi data showed a value equal to or lower than -2.00
402 (Figure 4). Moreover, 24% (12 events) of the episodes occurred in a negative (-
403 2.00, -1.00] WeMO phase. The remaining 8 events (16%) took place in a slightly
404 negative (-1.00, 0.00) WeMO phase. No extreme torrential episodes presenting
405 a positive WeMOi value occurred in Catalonia during the study period.
406 Furthermore, Martin-Vide and Lopez-Bustins (2006) found no positive daily
407 WeMOi values for torrential episodes (≥ 100 m in 24 h) in Tortosa (south
408 Catalonia) during the 1951-2000 period. On the other hand, the maximum
409 concentration of extreme torrential events according to NAOi values falls within
410 the interval (-1.00, 0.00), and both negative and positive NAOi values can account
411 for an event. This result demonstrates the fact that daily WeMOi values are more

412 useful than daily NAOi values. This is further evidenced by the fact that only 24%
 413 of the total number of events took place during an extreme negative (≤ -2.00) NAO
 414 phase, whereas this percentage rises to 60% in an extreme negative WeMO
 415 phase.

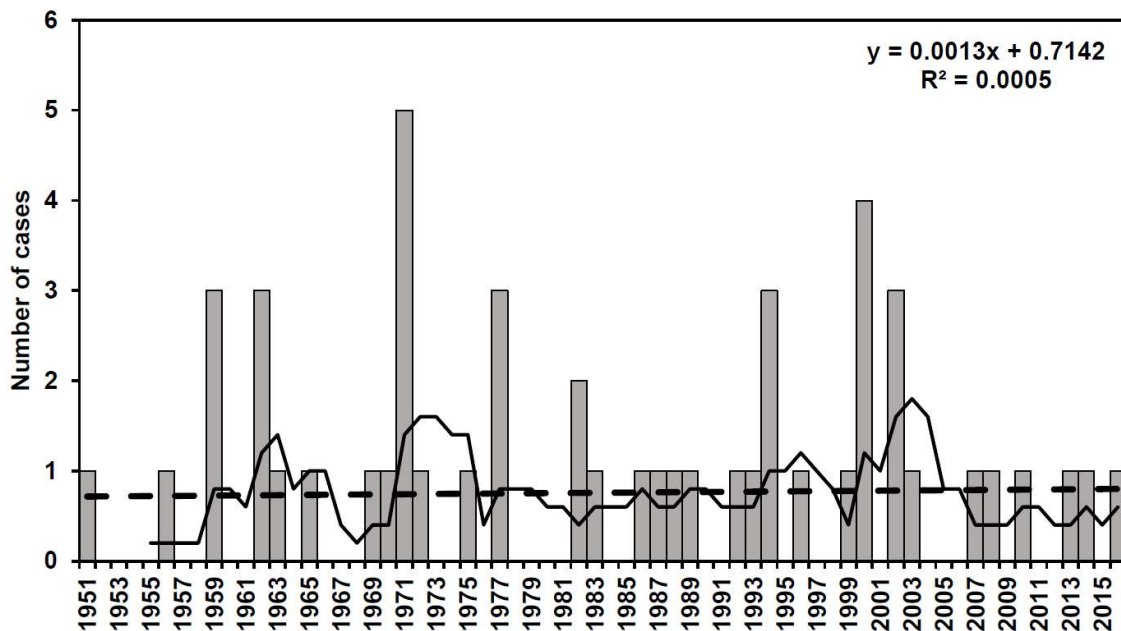


416

417 Figure 5. Frequency histogram of the daily WeMOi and NAOi values of the 50
 418 extreme torrential events recorded in Catalonia during the 1951-2016 study period.

419 Most of the years in the 1951-2016 period present no episodes, or only one (Figure 6);
 420 in six years there were 2 or 3 episodes, depending on the year, and in just two
 421 years (1971 and 2000) we detected over 3 episodes in one year. The greatest
 422 accumulation of cases can be observed in 1971, when a long-lasting torrential
 423 episode exceeded the threshold of 200 mm in 24 h during four consecutive days
 424 in September, with another one-day episode occurring in October. The former is
 425 one of the most noteworthy episodes recorded in Catalonia (Llasat, 1990; Martin-
 426 Vide and Llasat, 2000) in the last few decades. It started on September 19th in
 427 southern Catalonia and ended on September 22nd in the northeast of the study
 428 area (Llasat *et al.*, 2007). During the last decade, there has been no more than
 429 one episode in one single year. However, for torrential events (≥ 100 mm in 24 h)
 430 in Catalonia, Lopez-Bustins *et al.* (2016) detected a 45% increase in cases

431 between the 1950-1981 and 1982-2013 subperiods. In accordance with this rise
 432 in torrential precipitation events, many studies on Iberian precipitation are
 433 showing an increase in precipitation of Mediterranean origin in eastern Spain
 434 (Miró *et al.*, 2009; Lopez-Bustins *et al.*, 2008; De Luis *et al.*, 2010); this
 435 contributes to an increase in precipitation variability over the Western
 436 Mediterranean (Hartmann *et al.*, 2013, Caloiero *et al.*, 2019). On the other hand,
 437 non-statistical temporal trend is observed in the annual frequency of the extreme
 438 torrential episodes (i.e. ≥ 200 mm in 24 h) in Catalonia during the study period
 439 (Figure 6). This is in line with Llasat *et al.* (2016), who found non-statistical
 440 temporal trends in extreme daily precipitation in Catalonia.



441

442 Figure 6. Temporal evolution of the annual frequency of extreme torrential events
 443 (≥ 200 mm in 24 h) throughout the 1951-2016 study period. The figure shows the
 444 linear regression (dashed line) and 5-yr running mean (black line).

445 **4.2. Calendars of the daily WeMOi values**

446 The lowest WeMOi values are detected in autumn, especially in October (-0.38)
 447 (Figure 7a), usually with humid easterly flows from the Mediterranean Sea. This
 448 explains why autumn and October are the wettest season and month,
 449 respectively, on most of Spain's eastern façade (De Luis *et al.*, 2010). The
 450 greatest accumulation of extreme torrential events in Catalonia is in October, with
 451 19 events (38% of all cases). This is coherent with subsurface sea temperature,

452 which reaches its annual maximum in autumn (not shown). September also
453 shows a remarkable accumulation of events (11 cases), displaying the second
454 lowest WeMOi monthly value (-0.29). Positive WeMOi values are observed from
455 December to March, with very few events occurring. Sea temperature decreases
456 after the wet season, and the first months of the year constitute the period when
457 sea waters are the coldest (not shown). Additionally, WeMOi values are very high
458 in January and February, and the precipitation-convection phenomenon can
459 therefore be halted by a strong decrease in SST (Lebeaupin *et al.*, 2006).
460 Although negative WeMOi values are detected from April to November, very few
461 episodes are registered in late spring and summer; the predominance of
462 atmospheric stability during the warm season reduces the chances of extreme
463 torrential events occurring over the study area. At the fortnightly timescale, we
464 detected the minimum WeMOi value (-0.39) during the second half of October
465 (Figure 7b). The greatest accumulation of episodes, however, is in the first half
466 of October. The lowest WeMOi values are found from September 16th to October
467 31st. This short period of the year (46 days) accumulates over one half of the
468 total amount of extreme torrential events (28 cases, 56%). The most positive
469 WeMOi values are detected in the winter months, particularly from January 1st to
470 February 15th, and only 2 episodes are registered.

471 At the 10-day timescale, we observed the WeMOi minimum value (-0.45) from
472 October 11th to 20th (Figure 7c). This 10-day period also presents the largest
473 accumulation of extreme torrential events in Catalonia (8 cases; 16% of the total
474 number of cases). At least 4 cases are registered in each 10-day period from
475 September 11th to November 10th. This period of the year (61 days) accumulates
476 two thirds (33 cases, 66%) of all extreme torrential events. WeMOi values are
477 lower than -0.20 from August 1st to November 10th, fitting well with the period of
478 highest frequency of extreme torrential events in Catalonia. From August 1st to
479 September 10th, only 2 cases are registered due to the above-mentioned
480 atmospheric conditions in summer. From September 11th to November 10th,
481 favourable conditions can arise for the occurrence of extreme torrential events in
482 Catalonia: a high SST in the Western Mediterranean Sea and the early cut-off of
483 subpolar lows travelling to Mediterranean latitudes (Estrela *et al.*, 2008; Lopez-
484 Bustins, *et al.*, 2016; Pérez-Zanón *et al.*, 2018). The positive WeMOi values are

485 observed from December to March and each 10-day period presents either no
486 episode or only a single one. The most positive WeMOi value is observed from
487 January 1st to 10th (+0.38); this indicates the total predominance of the positive
488 phase of the teleconnection during these days, according to the 1951-2016 study
489 period (Figure 8a). During this 10-day period, the occurrence of extreme torrential
490 events in eastern Iberia is strongly inhibited by the NW atmospheric circulation
491 over the study area; sea waters are cold and the Genoa low is well represented.
492 The remaining 10-day periods in winter also present a predominance of the
493 western circulation over the Iberian Peninsula. This pattern causes positive
494 pressure differences between the Gulf of Cadiz (at a lower latitude) and the North
495 of Italy (at a higher latitude), which produces positive WeMOi values and inhibits
496 precipitation in eastern Iberia because of its location in the lee of the westerlies.
497 On the other hand, the mean sea level pressure (SLP) map from October 11th –
498 20th shows a predominance of the negative WeMO phase, with humid easterly
499 flows over Iberia, low pressure usually located in the Western Mediterranean
500 basin, and a blocking anticyclone over Central and Eastern Europe (Figure 8b).

501 This is approximately 60% of the year falling under negative WeMOi values at
502 monthly $N=8$ (out of 12) (Figure 7d), fortnightly $N=14$ (out of 24) (Figure 7e),
503 and 10-day $N=23$ (out of 36) (Figure 7f) timescales. The linear regression
504 between negative WeMOi values and episodes is statistically significant at all
505 timescales, providing an R of -0.73 (Figure 7d), -0.72 (Figure 7e) and -0.72
506 (Figure 7f). There is a statistically significant increase in the occurrence of events
507 as the WeMOi value decreases. The linear fitting is especially significant at 10-
508 day resolution.

509

510

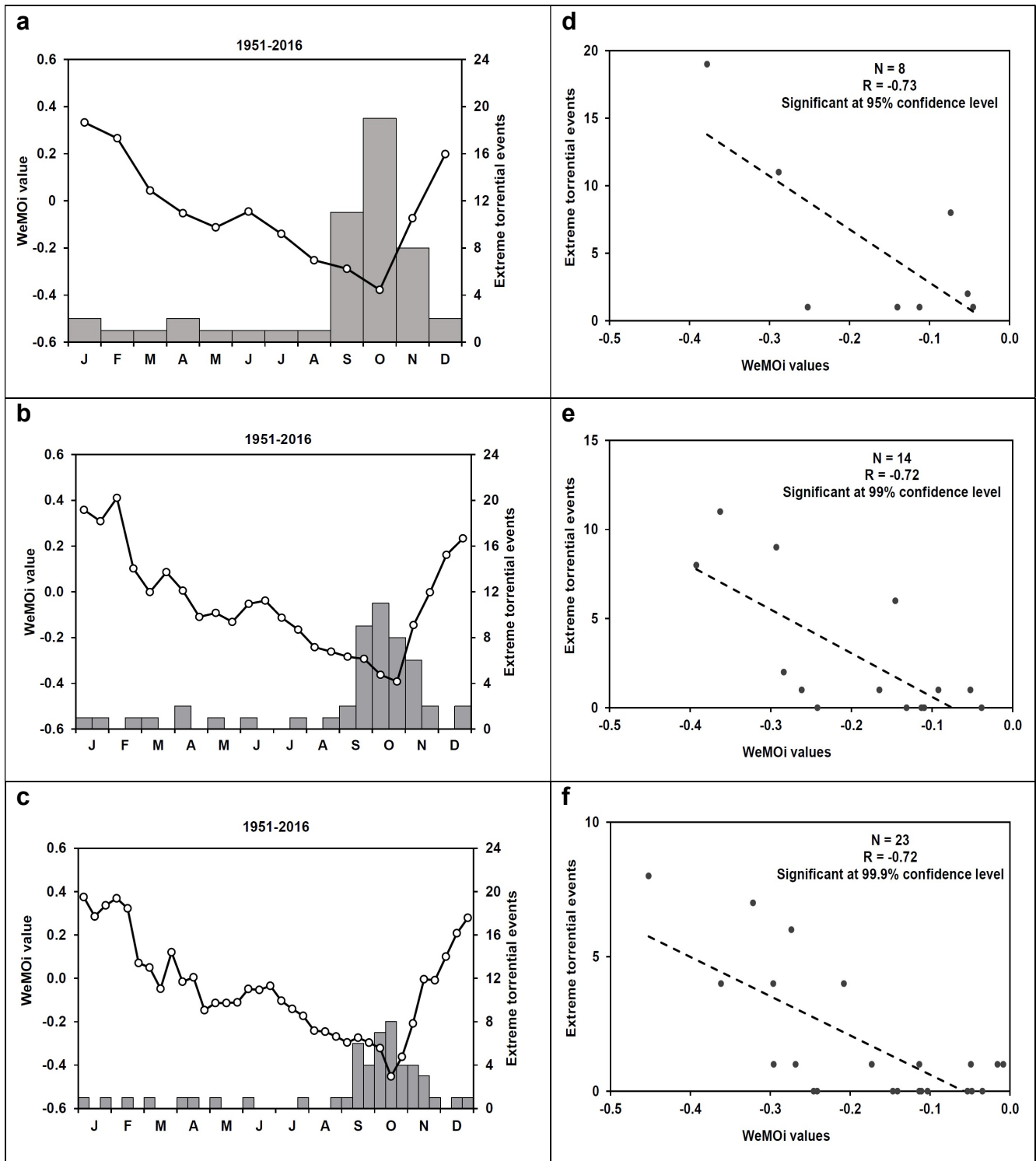
511

512

513

514

515

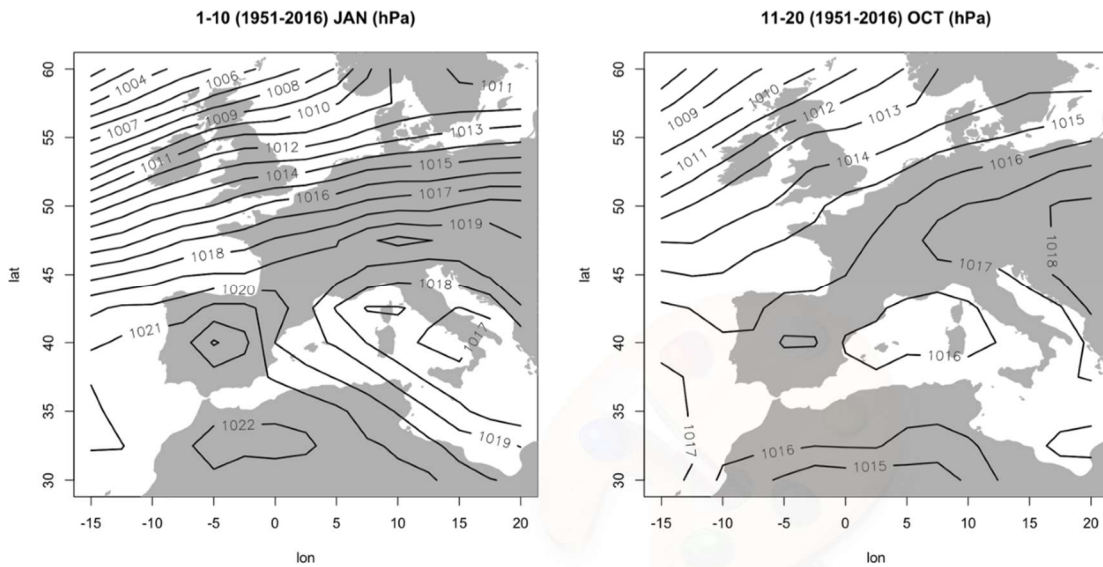


516 Figure 7. WeMOi calendars (lines) and frequency of extreme torrential episodes
 517 (bars) at several timescales: monthly (a), fortnightly (b) and 10-day (c).
 518 Scatterplot of the relationship between extreme torrential events and negative
 519 WeMOi values at several timescales: monthly (d), fortnightly (e) and 10-day (f);
 520 (the linear regression is shown as a dashed line).

522

(a)

(b)



523

524 Figure 8. Sea level pressure (SLP) mean of the synoptic window 30°N-60°N and
525 15°W-20°E from January 1st to 10th (a) and from October 11th to 20th (b) during
526 the 1951-2016 study period. Data source: NCEP Reanalysis data provided by the
527 NOAA/OAR/ESRL PSD, Boulder, Colorado, USA.

528 The WeMO teleconnection pattern can exert its influence upon precipitation
529 variability in other regions of Southern Europe (Caloiero *et al.*, 2011; Milosevic *et*
530 *al.*, 2016; Mathbout *et al.*, 2020). This central period of October may be the most
531 prone to torrential events over many regions of the western Mediterranean due
532 to presenting the lowest WeMOi value of the year. On the Iberian Peninsula, the
533 Almanzora river (SE Spain) suffered 2 of the 4 most catastrophic floods in the last
534 450 years within this central interval in October (Sánchez-García *et al.*, 2019).
535 Moreover, the deadliest torrential episodes in the Valencia Region (E Spain)
536 occurred on October 13th-14th 1957 and October 19th-20th 1982 (Olcina *et al.*,
537 2016; Miró *et al.*, 2017).

538

539 4.3. Subperiods and differences in the calendars

540 In relation to the calendars, and according to subperiods, we observed an overall
541 decrease in WeMOi values throughout the year (Figure 9). On the contrary, no
542 change was observed in the frequency of episodes between both subperiods;

543 exactly 25 extreme torrential events occurred in each subperiod. At the monthly
544 timescale, the extreme torrential period takes place in September and October
545 during the first half (1951-1983). For the second half (1984-2016), the maximum
546 accumulation of cases shifts from September-October to October-November,
547 with the highest concentration of cases in October, whilst new cases occur during
548 early winter (December). All WeMOi values are statistically and significantly lower
549 during the second subperiod than during the first one in all months, especially
550 from October to December. In the summer months, the decrease in WeMOi
551 values is moderate, albeit statistically significant due to the low variability of the
552 WeMOi values during the warm months. All these seasonal changes can be
553 related to trends in SST during the last few decades; the highest rate of SST
554 warming is in November (0.42 °C per decade) (Table 2). Higher SST is directly
555 associated both with a high rate of sea water evaporation and with more intense
556 latent heat transfer to the atmosphere (Pastor *et al.*, 2015), which is necessary
557 with regard to greatly increasing the precipitable water in the column. A general
558 warming of sea temperature has occurred along the year at all levels (SST, 20,
559 50, and 80 m.b.s.l.), particularly in spring, late autumn and early winter, a fact
560 which might explain these more negative WeMOi values during the second
561 subperiod; the warming of the lowest level of the atmosphere over the Western
562 Mediterranean Sea contributes to the formation of mesoscale lows (Jansà *et al.*,
563 2000). Similar rates of warming at near-surface sea level have been recorded in
564 other locations in the north Mediterranean Sea (Raicich and Colucci, 2019). The
565 highest warming rates have been observed at SST and 20 m.b.s.l., but the
566 statistical significance has been greater at the deepest levels, i.e. 50 and 80
567 m.b.s.l. (Table 2). Figure 10 shows that changes in WeMOi values between both
568 subperiods are negatively and statistically correlated with sea temperature
569 trends, above all, in the underlying layers, especially at 80 m.b.s.l., where sea
570 temperature displays a low interannual and intra-annual variability and sea heat
571 content hardly varies (Sparnocchia *et al.*, 2006).

572 At the fortnightly timescale, a shifting of maximum torrentiality is observed from
573 September 16th – October 15th to October 1st – October 31st. The lowest WeMOi
574 value of the calendar from 1951 to 1983 was in the first fortnight of October (-
575 0.26); however, the lowest value is observed in the second fortnight of October

576 during the 1984-2016 period (-0.58). All WeMOi values according to fortnights
577 showed a statistical and significant decrease during the second period, except
578 from January 16th to March 15th. The sharpest decline in WeMOi values is in the
579 first fortnight of May, the second fortnight of October, the second fortnight of
580 November and the first fortnight of December. The lowest WeMOi value during
581 the second subperiod is detected in the second fortnight of October, when the
582 greatest increase in extreme torrential events is observed.

583 At the 10-day timescale the lowest WeMOi values remain relatively constant from
584 the end of August to the beginning of November during the first subperiod, which
585 corresponds well with the occurrence of extreme torrential events. During the
586 second subperiod, the lowest WeMOi values are found from October 11th to 31st,
587 with an accumulation of 8 cases (32% of the total number of cases of the second
588 subperiod). A continuous and statistically significant decrease in WeMOi values
589 (at the 99.9% confidence level) is observed from October 16th to December 20th
590 during the second subperiod, except for the first 10-day period of November. The
591 increase in torrential events is especially concentrated from October 21st to 31st.
592 From August 21st to October 10th there is an overall decline in extreme torrential
593 events, which might be associated with the fact that the WeMOi values hardly
594 show a decrease over these 10-day periods of the year during the second
595 subperiod. This is in line with the fact that the warming was moderate, or that
596 there was even a certain degree of cooling, during the first 10-day periods of the
597 wet season, i.e. from September 1st to October 20th, in the underlying sea layers
598 (Table 3); and consequently, episodes might not have been favoured during the
599 second subperiod. The highest sea temperature increase at all levels during the
600 wet season is in the third 10-day period of October (Table 3), when the highest
601 increase in extreme torrential episodes is observed (Figure 9). The changes in
602 the frequency of episodes are statistically correlated with sea temperatures at
603 subsurface layers, i.e. 50 and 80 m.b.s.l. (Figure 11). The deepest level (80
604 m.b.s.l.) shows the strongest warming in late autumn (from October 21st to
605 November 30th), whereas this warming is weak in early autumn (from September
606 1st to October 20th) (Figure 12). This could be related to some recent changes
607 in thermocline depth and time of destruction thereof due to warming of the
608 Mediterranean Sea over the last few decades (Salat *et al.*, 2019). The subsurface

609 temperature may show a more constant warming of the Mediterranean Sea than
610 SST, because the latter is usually affected by local phenomena.

611 In general terms, no more cases of extreme torrential events are observed during
612 the 1984-2016 period in comparison with the 1951-1983 period. Nonetheless, a
613 greater accumulation of cases can be observed during late autumn and a lesser
614 accumulation in early autumn during the second subperiod, in comparison with
615 the first one. A sharp and continuous drop in WeMOi values is observed at the
616 very end of autumn, which might indicate a shift in the seasonality of the extreme
617 torrential period from September-October to October-November and an increase
618 in precipitation irregularity due to a deeper WeMO negative phase (Lopez-Bustins
619 and Lemus-Canovas, 2020). This seasonal shifting might be caused by a recent
620 increase in sea temperature in the Western Mediterranean basin, particularly in
621 November (Table 2) and late October (Table 3) (Lopez-Bustins, 2007; Estrela *et*
622 *al.*, 2008; Lopez-Bustins *et al.*, 2016; Arbiol-Roca *et al.*, 2017). Pastor *et al.*
623 (2018) used satellite data to identify an overall increase in SST throughout the
624 Mediterranean basin during the 1982-2016 period, highlighting its role in torrential
625 events in the Western Mediterranean.

626

627

628

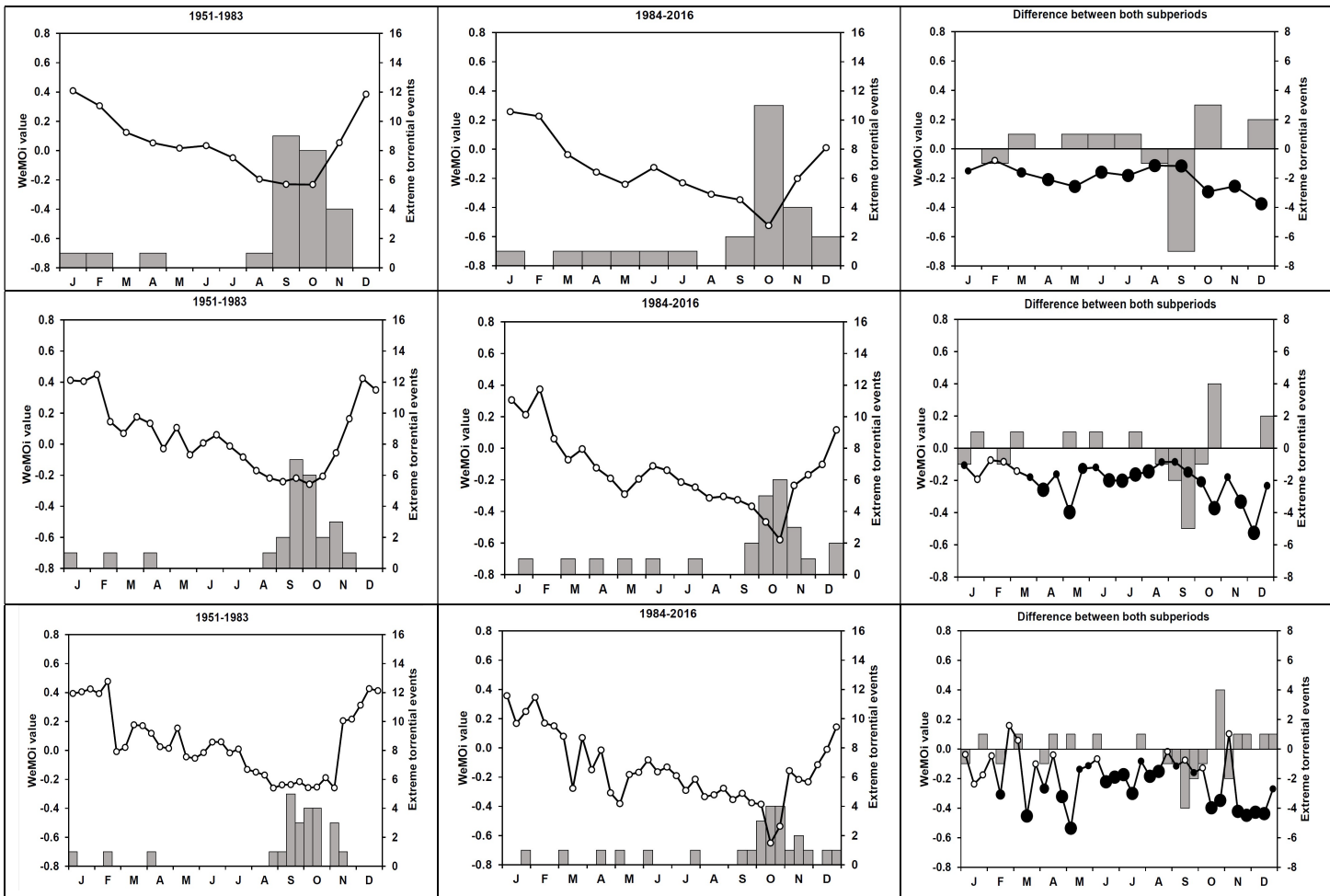
629

630

631

632

633



634 Figure 9. WeMOi calendars (lines) and frequency of extreme torrential episodes
 635 (bars) at several timescales: monthly (above), fortnightly (middle) and
 636 (below) for the 1951-1983 (left) and 1984-2016 (central) subperiods. The right-
 637 hand column shows the difference in the number of episodes and WeMOi values
 638 between both subperiods (for WeMOi values: white dots indicate not statistically
 639 significant differences, and small-, medium- and large-sized black dots show
 640 statistically significant differences at the 95.0%, 99.0% and 99.9% confidence
 641 levels, respectively).

642

643

644

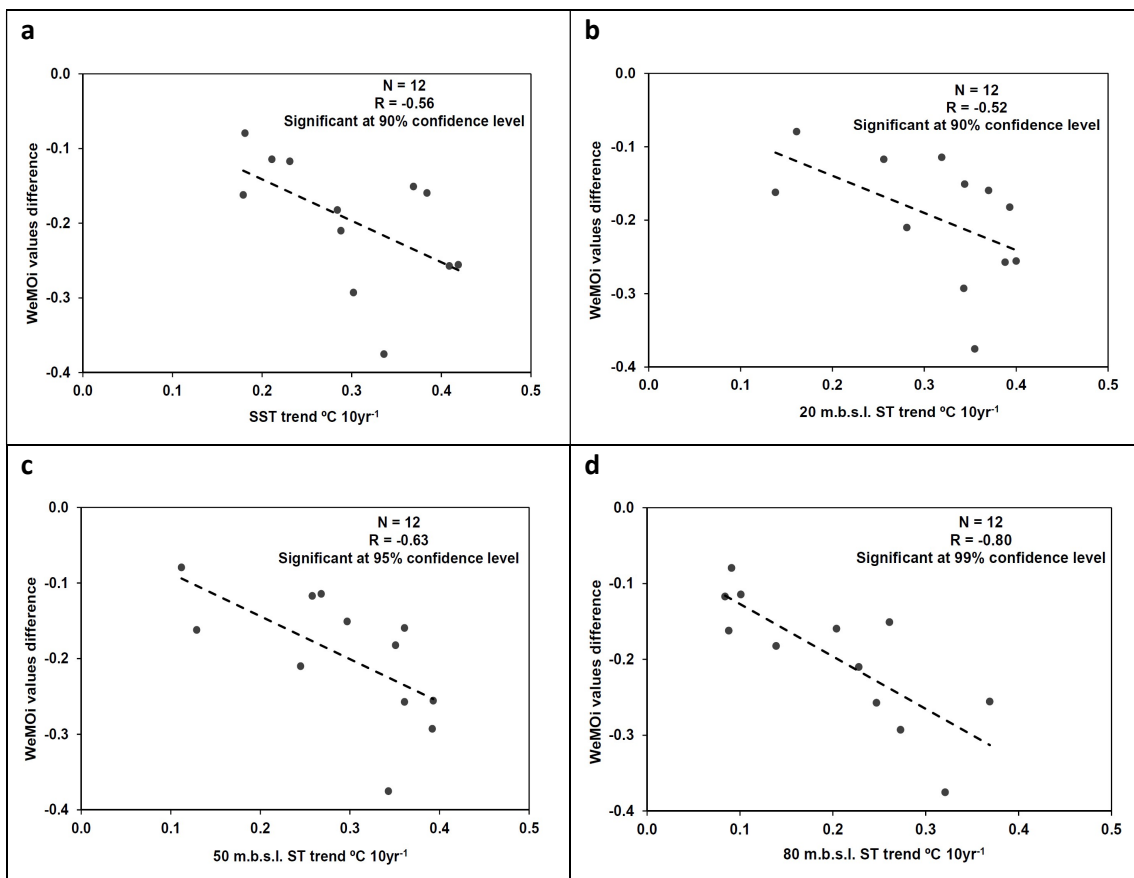
645

646

N = 44 1973-2016		J	F	M	A	M	J	J	A	S	O	N	D	°C 10yr ⁻¹	
SST	*	*	*	*	*	*	*	*	*	*	*	*	*	<0.15	0.30-0.34
-20 m	*	*		*	*	*	*	*	*	*	*	*	*	0.15-0.19	0.35-0.39
-50 m	*			*	*	*	*	*	*	*	*	*	*	0.20-0.24	≥0.40
-80 m	*			*	*	*	*	*	*	*	*	*	*	0.25-0.29	

647 Table 2. Monthly sea temperature trends at surface (SST), 20, 50, and 80 m.b.s.l.
 648 during 1973-2016 (*statistically significant trends at the 95% confidence level by
 649 means of the Mann-Kendall non-parametric test).

650



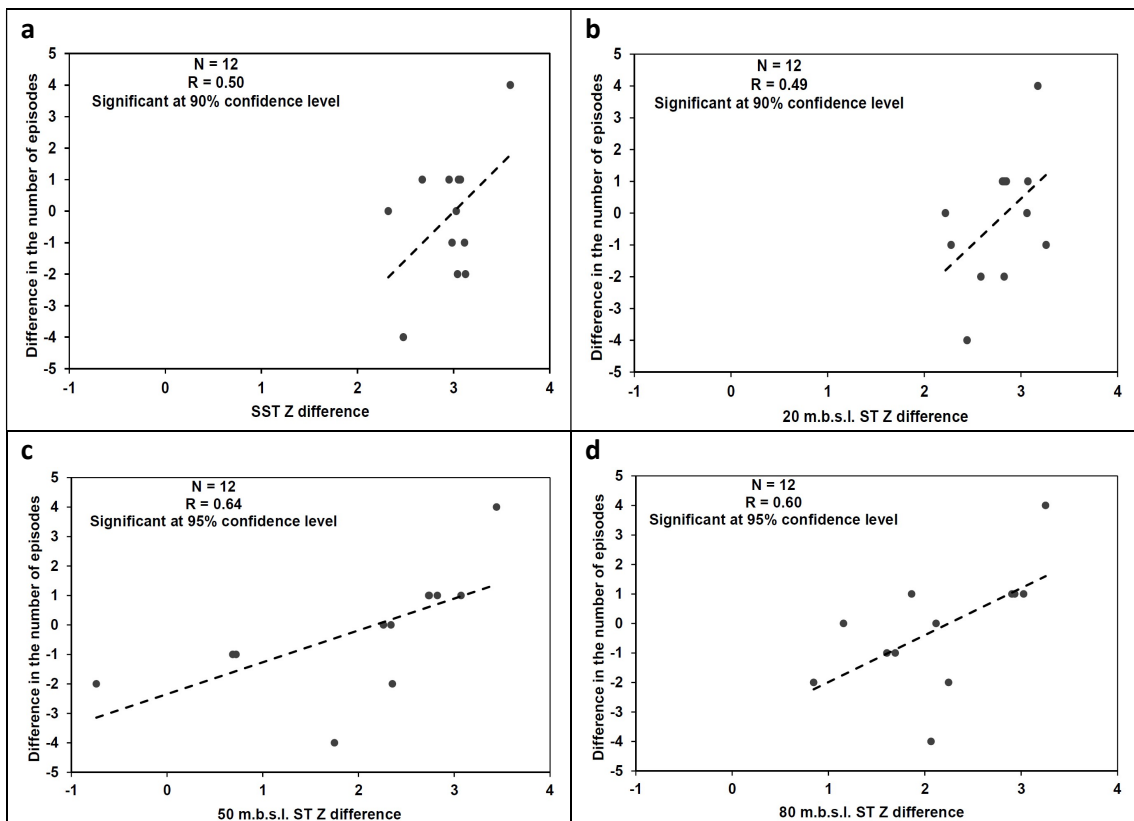
651 Figure 10. Scatterplot of the monthly relationship between the WeMOi value
 652 differences (1984-2016 minus 1951-1983) and sea temperature (ST) trends
 653 during the 1973-2016 period at surface (SST) (a), 20 (b), 50 (c), and 80 (d)
 654 m.b.s.l. (a dashed line indicates the linear regression).

655
 656
 657
 658
 659
 660

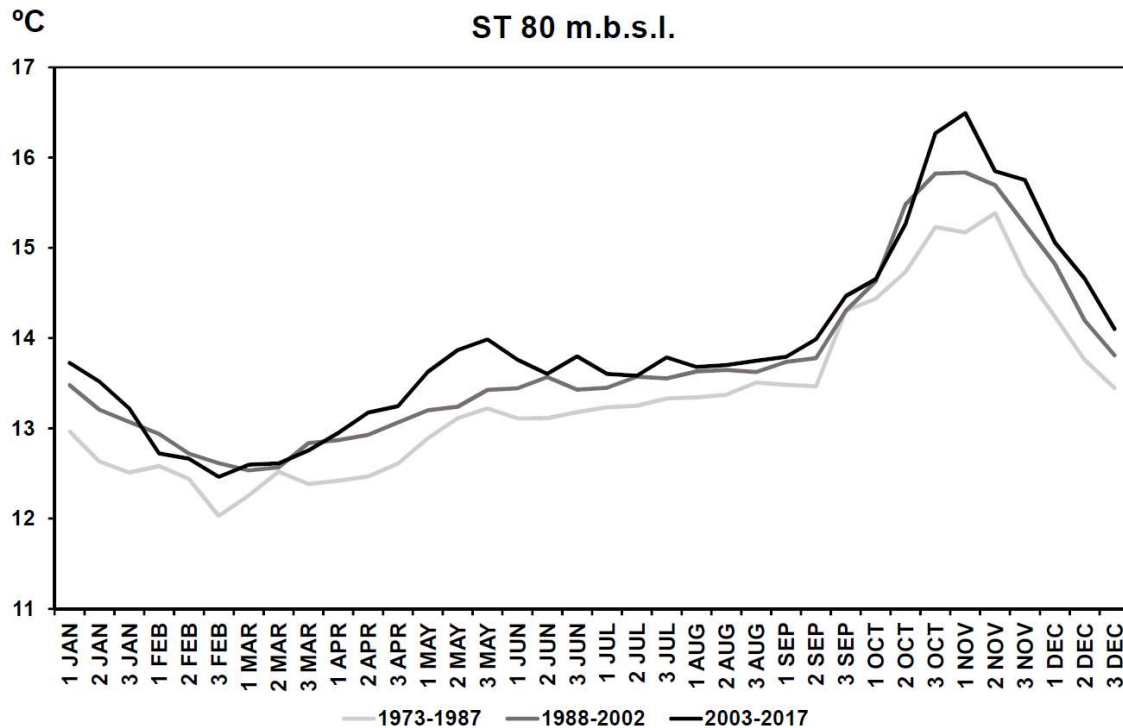
	1	2	3	1	2	3	1	2	3	1	2	3	Z	
	SEP	SEP	SEP	OCT	OCT	OCT	NOV	NOV	NOV	DEC	DEC	DEC	<0.00	
SST													0.00-0.49	2.00-2.49
-20 m													0.50-0.99	2.50-2.99
-50 m													1.00-1.49	3.00-3.49
-80 m													1.50-1.99	≥3.50

661 Table 3. 10-day period ST standardized values (Z) differences for two 5-yr
662 subperiods (2013-2017 minus 1973-1977) at surface, 20, 50, and 80 m.b.s.l.
663 during the wet season (from September to November) and December.

664



665 Figure 11. Scatterplot of the 10-day relationship between the differences in the
666 number of episodes (1984-2016 minus 1951-1983) and ST Z differences for two
667 5-yr subperiods (2013-2017 minus 1973-1977) at surface (a), 20 (b), 50 (c), and
668 80 (d) m.b.s.l. during the wet season (from September to November) and
669 December (a dashed line indicates the linear regression).



670

671 Figure 12. ST 10-day calendar at 80 m.b.s.l. for three 15-yr subperiods: 1973-

672 1987, 1988-2002 and 2003-2017.

673 **5. Conclusions**

674 The present research confirms the usefulness of the WeMOi at daily resolution
 675 as an effective tool for analysing the occurrence of episodes of torrential
 676 precipitation over NE Spain. October is the rainiest month in most regions of the
 677 Northwestern Mediterranean basin and can account for the lowest value of the
 678 year on the WeMOi monthly calendar, together with the warmest sea temperature
 679 of the year at subsurface level. Moreover, most torrential episodes take place
 680 during a very short period in the middle of this month.

681 Catalonia is located in the Northwestern Mediterranean basin and its extreme
 682 precipitation is highly dependent upon the atmospheric circulation over the
 683 Mediterranean. The present study considers the threshold of 200 mm in 24 h for
 684 extreme torrential episodes, due to the fact that this precipitation accumulation in
 685 one day can cause serious widespread damage over a large area. Having
 686 thoroughly reviewed several databases and contrasted these results with the
 687 original files and nearby weather stations, we confirmed that Catalonia registered

688 0.8 cases per year (50 episodes in 66 years) of extreme torrential episodes during
689 the 1951-2016 study period, in accordance with the 7-7 UTC pluviometric day.

690 The 10-day period from October 11th to 20th exhibits both the greatest
691 accumulation of extreme torrential episodes in Catalonia and the lowest intra-
692 annual WeMOi value. This 10-day period has been demonstrated to be the most
693 prone to torrential events in this Northwestern Mediterranean area, according to
694 the WeMOi values. The most intense torrential event in Catalonia ever recorded
695 by an official weather station is in Cape Creus (the easternmost part of the Iberian
696 Peninsula) within the 10-day period most susceptible to torrential precipitation
697 (October 13th 1986), with a total amount of 430 mm. The most positive WeMO
698 phase of the year usually takes place in January, especially from January 1st to
699 10th, when the synoptic and sea temperature conditions of this time of the year
700 inhibit torrential events.

701 No extreme torrential episodes in Catalonia occurred in a positive WeMO phase.
702 Additionally, 60% of the cases occurred in an extreme negative WeMO phase,
703 i.e. a WeMOi value equal to or lower than -2.00. In the present study this threshold
704 is considered to constitute the onset of a rainstorm favoured by a strong
705 Mediterranean flow. The lower WeMOi value is related to an increase in extreme
706 torrential events at all timescales. On comparing both study subperiods (1951-
707 1983 and 1984-2016), an overall statistically significant decrease is detected in
708 most WeMOi values of the year, especially at the end of October and some
709 periods in November and December. This might have been caused by an overall
710 increase in sea temperature throughout the year, particularly in late autumn; **this**
711 **sea warming can enhance air convection (a decrease in surface pressure) over**
712 **the Western Mediterranean basin**. On the other hand, extreme torrential events
713 show no changes in frequency between both subperiods; no temporal trend is
714 observed, either, during the 1951-2016 study period. The most notable change
715 involves the displacement of extreme torrential episodes from early to late
716 autumn; this is in accordance with the lower WeMOi values detected in the last
717 three months of the year during the second subperiod. Increases in sea
718 temperatures in the underlying layers during the end of the wet season can
719 provide an understanding of these changes in extreme torrential events and in
720 the WeMOi calendars. **Sea temperature is an additional factor influencing**

721 torrential episodes in Catalonia; higher (lower) precipitation amounts can be
722 registered in accordance with warmer (colder) than normal sea waters
723 (Lebeaupin *et al.*, 2006). The main causes of heavy precipitation in Catalonia
724 involve easterly humid flows at surface level with an upper cut-off low (Martin-
725 Vide *et al.*, 2008), and troughs in the upper troposphere with an advection
726 maximum of positive vorticity on their front edge (Lolis and Türkeş, 2016).

727

728 **Data availability**

729 The WeMOi data can be downloaded from the Climatology Group (University of
730 Barcelona) website <http://www.ub.edu/gc/en/> (last accessed July 5th 2020).

731 **Author contributions**

732 JALB performed the analysis and wrote the paper. LAR updated the WeMOi data
733 and plotted the pressure maps. JMV discussed the results. ABE elaborated the
734 inventory of the episodes and discussed the results. MPD discussed the results.

735 **Competing interests**

736 The authors declare that they have no conflict of interest.

737 **Acknowledgments**

738 The present study was conducted within the framework of the Climatology Group
739 of the University of Barcelona (2017 SGR 1362, Catalan Government) and the
740 CLICES Spanish project (CGL2017-83866-C3-2-R, AEI/FEDER, UE). Our
741 research benefited from the daily precipitation data provided by the
742 Meteorological Service of Catalonia. We are especially indebted to the
743 meteorological observer from l'Estartit (Girona province), Josep Pascual, who
744 painstakingly recorded sea temperature data over the last few decades.

745 **References**

746 Alfieri, L., Burek, P., Feyen, L., Forzieri, G., 2015. Global warming increases the
747 frequency of river floods in Europe. *Hydrology and Earth System Sciences* 19,
748 2247-2260. DOI: 10.5194/hess-19-2247-2015, 2015.

749 Arbiol-Roca, L., Lopez-Bustins, J.A., Martin-Vide, J.: The role of the WeMOi in
750 the occurrence of torrential rainfall in Catalonia (NE Iberia). Abstracts book: 6th
751 International Conference on Meteorology and Climatology of the Mediterranean
752 (MetMed). Zagreb (Croatia): ACAM, 2017.

753 Arbiol-Roca, L., Lopez-Bustins, J.A., Esteban-Vea, P., Martin-Vide, J.: Cálculo
754 del índice de la Oscilación del Mediterráneo Occidental con técnicas de análisis
755 multivariante. In: Montávez-Gómez, J.P., Gómez-Navarro, J.J., López-Romero,
756 J.M., Palacios-Peña, L., Turco, M., Jerez-Rodríguez, S., Lorente, R., Jiménez-
757 Guerrero, P. (eds.), El Clima: Aire, Agua, Tierra y Fuego, pp. 761-771. Cartagena
758 (Spain): Asociación Española de Climatología (AEC), 2018.

759 Armengot, R.: Las lluvias intensas en la Comunidad Valenciana. 263 pp. Madrid
760 (Spain): Ministerio de Medio Ambiente, Dirección General del Instituto Nacional
761 de Meteorología, 2002.

762 Azorin-Molina, C., Lopez-Bustins, J.A.: An automated sea breeze selection
763 based on regional sea-level pressure difference: WeMOi. International Journal of
764 Climatology 28, 1681-1692. DOI: 10.1002/joc.1663, 2008.

765 Baldwin, M.P., Dunkerton T.J.: Stratospheric harbingers of anomalous weather
766 regimes. Science 294, 581-584. DOI: 10.1126/science.1063315, 2001.

767 Barrera-Escoda, A., Gonçalves, M., Guerreiro, D., Cunillera, J., Baldasano, J.M.:
768 Projections of temperature and precipitation extremes in the North Western
769 Mediterranean Basin by dynamical downscaling of climate scenarios at high
770 resolution (1971-2050). Climate Change 122, 567-582. DOI: 10.1007/s10584-
771 013-1027-6, 2014.

772 Beguería, S., Angulo-Martínez, M., Vicente-Serrano, S.M., López-Moreno, J.I.,
773 Kenawy, A.: Assessing trends in extreme precipitation events intensity and
774 magnitude using non-stationary peaks-over-threshold analysis: a case study in
775 northeast Spain from 1930 to 2006. International Journal of Climatology 31, 2102-
776 2114. DOI:10.1002/joc.2218, 2011.

777 Beniston, M., Junco, P.: Shifts in the distributions of pressure, temperature and
778 moisture in the Alpine region in response to the behaviour of the North Atlantic

779 Oscillation. *Theoretical and Applied Climatology* 71, 29-42. DOI: 10.1007/s704-
780 002-8206-7, 2002.

781 Caloiero, T., Coscarelli, R., Ferrari, E., Mancini, M.: Precipitation change in
782 Southern Italy linked to global scale oscillation indexes. *Natural Hazards and*
783 *Earth System Sciences* 11, 1683-1694. DOI: 10.5194/nhess-11-1683-2011,
784 2011.

785 Caloiero, T., Coscarelli, R., Gaudio, R.: Spatial and temporal variability of daily
786 precipitation concentration in the Sardinia region (Italy). *International Journal of*
787 *Climatology* 39, 5006–5021, 2019.

788 Christensen, J.H., Krishna Kumar, K., Aldrian, E., An, S.-I., Cavalcanti, I.F.A., de
789 Castro, M., Dong, W., Goswami, P., Hall, A., Kanyanga, J.K., Kitoh, A., Kossin,
790 J., Lau, N.-C., Renwick, J., Stephenson, D.B., Xie, S.-P., Zhou, T.: Climate
791 Phenomena and their Relevance for Future Regional Climate Change. In:
792 *Climate Change 2013: The Physical Science Basis. Contribution of Working*
793 *Group I to the Fifth Assessment Report of the Intergovernmental Panel on*
794 *Climate Change* [Stocker, T.F., D. Qin, G.-K. Plattner, M. Tignor, S.K. Allen, J.
795 Boschung, A. Nauels, Y. Xia, V. Bex and P.M. Midgley (eds.)]. Cambridge
796 University Press, Cambridge, UK and New York, NY, USA. DOI:
797 10.1017/CBO9781107415324.028, 2013.

798 Coll, M., Carreras, M., Ciércoles, C., Cornax, M.J., Gorelli, G., Morote, E., Sáez,
799 R.: Assessing fishing and marine biodiversity changes using fishers' perceptions:
800 the Spanish Mediterranean and Gulf of Cadiz case study. *PLoS ONE* 9(1):
801 e85670. DOI: 10.1371/journal.pone.0085670, 2014.

802 Cornes, R., van der Schrier, G., van den Besselaar, E.J.M., Jones, P.D.: An
803 Ensemble Version of the E-OBS Temperature and Precipitation Datasets.
804 *Journal of Geophysical Research: Atmospheres* 123, 9391-9409. DOI:
805 10.1029/2017JD028200, 2018.

806 Cortesi, N., Gonzalez-Hidalgo, J.C., Brunetti, M., Martin-Vide, J.: Daily
807 precipitation concentration across Europe 1971-2010. *Natural Hazards and Earth*
808 *System Sciences* 12, 2799-2810. DOI: 10.5194/nhess-12-2799-2012, 2012.

809 Cramer, W., Guiot, J., Fader, M., Garrabou, J., Gattuso, J.P., Iglesias, A., Lange,
810 M.A., Lionello, P., Llasat, M.C., Paz, S., Peñuelas, J., Snoussi, M., Toreti, A.,
811 Tsimplis, M.N., Xoplaki, E.: Climate change and interconnected risks to
812 sustainable development in the Mediterranean. *Nature Climate Change* 8, 972–
813 DOI: 10.1038/s41558-018-0299-2, 2018.

814 De Luis, M., Brunetti, M., Gonzalez-Hidalgo, J.C., Longares, L.A., Martin-Vide, J.:
815 Changes in seasonal precipitation in the Iberian Peninsula during 1946-2005.
816 *Global and Planetary Change* 74, 27-33. DOI: 10.1038/s41558-018-0299-2,
817 2010.

818 El Kenawy, A., López-Moreno, J.I., Vicente-Serrano, S.M.: Trend and variability
819 of surface air temperature in northeastern Spain (1920-2006): Linkage to
820 atmospheric circulation. *Atmospheric Research* 106, 159-180. DOI:
821 10.1016/j.atmosres.2011.12.006, 2012.

822 Estrela, M.J., Pastor, F., Miró, J., Valiente, J.A.: Precipitaciones torrenciales en
823 la Comunidad Valenciana: La temperatura superficial del agua del mar y áreas
824 de recarga. Primeros resultados. In: M.J. Estrela Navarro (ed.), *Riesgos
825 climáticos y cambio global en el mediterráneo español ¿hacia un clima de
826 extremos?*, pp. 121-140. Valencia (Spain): Colección Interciencias, 2008.

827 Gil-Guirado, S., Pérez-Morales, A., Lopez-Martinez, F.: SMC-Flood database: a
828 high-resolution press database on flood cases for the Spanish Mediterranean
829 coast (1960–2015). *Natural Hazards and Earth System Sciences* 19, 1955-1971.
830 DOI: 10.5194/nhess-19-1955-2019, 2019.

831 Gilabert, J., Llasat, M.C.: Circulation weather types associated with extreme flood
832 events in Northwestern Mediterranean. *International Journal of Climatology*, 38,
833 1864-1876. DOI:10.1002/joc.5301, 2018.

834 González-Hidalgo, J.C., Lopez-Bustins, J.A., Stepanek, P. Martin-Vide, J., De
835 Luis, M.: Monthly precipitation trends on the Mediterranean fringe of the Iberian
836 Peninsula during the second-half of the twentieth century (1951-2000).
837 *International Journal of Climatology* 29, 415-1429. DOI: 10.1002/joc.1780, 2009.

838 González-Hidalgo, J. C., Brunetti, M., de Luis, M.: A new tool for monthly
839 precipitation analysis in Spain: MOPREDAS database (monthly precipitation

840 trends December 1945–November 2005). *International Journal of Climatology*
841 31, 715-731. DOI: 10.1002/joc.2115, 2011.

842 Greve, P., Gudmundsson, L., Seneviratne, S.I.: Regional scaling of annual mean
843 precipitation and water availability with global temperature change. *Earth System*
844 *Dynamics Discussion* 9, 227-240. DOI: 10.3929/ethz-b-000251688, 2018.

845 Holton, J.R.: *An Introduction to Dynamic Meteorology*. Elsevier Academic Press,
846 *International Geophysics Series*, volume 88, 4th edition, 535 pp, 2004.

847 Hartmann, D.L., Klein Tank, A.M.G., Rusticucci, M., Alexander, L.V.,
848 Brönnimann, S., Charabi, Y., Dentener, F.J., Dlugokencky, E.J., Easterling, D.R.,
849 Kaplan, A., Soden, B.J., Thorne, P.W., Wild, M., Zhai, P.M.: *Observations:*
850 *Atmosphere and Surface*. In: *Climate Change 2013: The Physical Science Basis.*
851 *Contribution of Working Group I to the Fifth Assessment Report of the*
852 *Intergovernmental Panel on Climate Change* [Stocker, T.F., D. Qin, G.-K.
853 Plattner, M. Tignor, S.K. Allen, J. Boschung, A. Nauels, Y. Xia, V. Bex and P.M.
854 Midgley (eds.)]. Cambridge University Press, Cambridge, United Kingdom and
855 New York, NY, USA. DOI: 10.1017/CBO9781107415324.008, 2013.

856 Iizuka, S., Nakamura, H.: Sensitivity of midlatitude heavy precipitation to SST: A
857 case study in the Sea of Japan area on 9 August 2013. *Journal of Geophysical*
858 *Research: Atmospheres*, 124, 4365–4381. DOI:10.1029/2018JD029503, 2019.

859 Jang, J.H.: An advanced method to apply multiple rainfall thresholds for urban
860 flood warnings. *Water* 7, 6056-6078. DOI: 10.3390/w7116056, 2015.

861 Jansà, A., Genovés, A.: Western Mediterranean cyclones and heavy rain. Part 1:
862 Numerical experiment concerning the Piedmont flood case. *Meteorological*
863 *Applications*, 7(4), 323-333. DOI:10.1017/S1350482700001663, 2000.

864 Jansà, A., Genovés, A., Riosalido, R., Carretero, O.: Mesoscale cyclones vs
865 heavy rain and MCS in the Western Mediterranean. *MAP newsletter*, 5, 24-25,
866 1996.

867 Jansà, A., Genovés, A., Picornell, M., Campins, J., Riosalido, R., Carretero, O.:
868 Western Mediterranean cyclones and heavy rain. Part 2: Statistical approach.
869 *Meteorological Applications*, 8(1), 43-56. DOI:10.1017/S1350482701001049,
870 2000.

871 Jghab, A., Vargas-Yañez, M., Reul, A., Garcia-Martínez, M.C., Hidalgo, M.,
872 Moya, F., Bernal, M., Ben Omar, M., Benchoucha, S., Lamtai, A.: The influence
873 of environmental factors and hydrodynamics on sardine (*Sardina pilchardus*,
874 Walbaum 1792) abundance in the southern Alboran Sea. *Journal of Marine*
875 *Systems* 191, 51-63. DOI: 10.1016/j.jmarsys.2018.12.002, 2019.

876 Klein Tank, A.M.G., Wijngaard, J.B., Können, G.P., Böhm, R., Demarée, G.,
877 Gocheva, A., Mileta, M., Pashiardis, S., Hejkrlik, L., Kern-Hansen, C., Heino, R.,
878 Bessemoulin, P., Müller-Westermeier, G., Tzanakou, M., Szalai, S., Pálsdóttir,
879 T., Fitzgerald, D., Rubin, S., Capaldo, M., Maugeri, M., Leitass, A., Bukatis,
880 A., Aberfeld, R., van Engelen, A.F.V., Forland, E., Miletus, M., Coelho, F., Mares,
881 C., Razuvaev, V., Nieplova, E., Cegnar, T., López, J.A., Dahlström, B., Moberg,
882 A., Kirchhofer, W., Ceylan, A., Pachaliuk, O., Alexander, L.V., Petrovic, P.: Daily
883 dataset of 20th-century surface air temperature and precipitation series for the
884 European climate assessment. *International Journal of Climatology* 22, 1441-
885 1453. DOI: 10.1002/joc.773, 2002.

886 Knoben, W.J.M., Woods, R.A., Freer, J.E.: Global bimodal precipitation
887 seasonality: A systematic overview. *International Journal of Climatology* 39, 558
888 - 567. DOI: 10.1002/joc.5786, 2019.

889 Kottek, M., Grieser, J., Beck, C., Rudolf, B., Rubel, F.: World Map of the Köppen-
890 Geiger climate classification updated. *Meteorologische Zeitschrift* 15, 259-263.
891 DOI: 10.1127/0941-2948/2006/0130, 2006.

892 Kreibich, H., Di Baldassarre, G., Vorogushyn, S., Aerts, J.C.J.H., Apel, H.,
893 Aronica, G.T., Arnbjerg-Nielsen, K., Bouwer, L.M., Bubeck, P., Caloiero, T.,
894 Chinh, D.T., Cortès, M. Gain, A.K., Giampá, V., Kuhlicke, C., Kundzewicz, Z.W.,
895 Llasat, M.C., Mård, J., Matczak, P., Mazzoleni, M., Molinari, D., Dung, N.V.,
896 Petrucci, O., Schröter, K., Slager, K., Thielen, A.H., Ward, P.J., Merz, B.:
897 Adaptation to flood risk: Results of international paired flood event studies.
898 *Earth's Future* 5, 953-965. DOI: 10.1002/2017EF000606, 2017.

899 Lana, X., Burgueño, A., Martínez, M.D., Serra, C.: Complexity and predictability
900 of the monthly Western Mediterranean Oscillation index. *International Journal of*
901 *Climatology* 36, 2435-2450. DOI: 10.1002/joc.4503, 2016.

902 Lana, X., Burgueño, A., Martínez, M.D., Serra, C.: Monthly rain amounts at Fabra
903 Observatory (Barcelona, NE Spain): fractal structure, autoregressive processes
904 and correlation with monthly Western Mediterranean Oscillation index.
905 International Journal of Climatology 37, 1557-1577. DOI: 10.1002/joc.4797,
906 2017.

907 Lebeaupin, C., Ducrocq, V., Giordani, H. Sensitivity of Mediterranean torrential
908 rain events to the sea surface temperature based on high-resolution numerical
909 forecasts. Journal of Geophysical Research 111, D12110.
910 doi:10.1029/2005JD006541, 2006.

911 Liu, Y.; Li, Z.; Yin, H.: A timely El Niño-Southern Oscillation forecast method
912 based on daily Niño index to ensure food security. Published in: 2018 7th
913 International Conference on Agro-geoinformatics (Agro-geoinformatics) DOI:
914 10.1109/Agro-Geoinformatics.2018.8476070, 2018.

915 Llasat, M.C.: Influencia de la orografía y de la inestabilidad convectiva en la
916 distribución espacial de lluvias extremas en Cataluña. Acta Geologica Hispanica
917 25, 197-208, 1990.

918 Llasat, M.C.: High magnitude storms and floods, in Woodwar, J.C. (ed.). The
919 Physical Geography of the Mediterranean. Oxford University Press, Oxford, UK,
920 513-540, 2009.

921 Llasat, M.C., Martín, F., Barrera, A.: From the concept of 'kaltlufttropfen' (cold air
922 pool) to the cut-off low. The case of September 1971 in Spain as an example of
923 their role in heavy rainfalls. Meteorology and Atmospheric Physics 96, 43-60.
924 DOI: 10.1007/s00703-006-0220-9, 2007.

925 Llasat, M.C., Marcos, R., Turco, M., Gilabert, J., Llasat-Botija, M.: Trends in flash
926 flood events versus convective precipitation in the Mediterranean region: The
927 case of Catalonia. Journal of Hydrology 541, 24-37. DOI:
928 10.1016/j.jhydrol.2016.05.040, 2016.

929 Lolis, C.J., Türkeş, M.: Atmospheric circulation characteristics favouring extreme
930 precipitation in Turkey. Climate Research 71, 139-153. DOI: 10.3354/cr01433,
931 2016.

932 Lopez-Bustins, J.A.: The Western Mediterranean Oscillation and Rainfall in the
933 Catalan Countries. PhD Thesis, Department of Physical Geography and Regional
934 Geographical Analysis, University of Barcelona, 184 pp, 2007.

935 Lopez-Bustins, J.A.: Lluvias fuertes, pero mal repartidas. El caso del clima
936 mediterráneo. Biblio3W Revista Bibliográfica de Geografía y Ciencias Sociales
937 vol. 23, no 1243, 2018.

938 Lopez-Bustins, J.A., Lemus-Canovas, M.: The influence of the Western
939 Mediterranean Oscillation upon the spatiotemporal variability of precipitation over
940 Catalonia (northeastern of the Iberian Peninsula). Atmospheric Research 236,
941 104819, DOI: 10.1016/j.atmosres.2019.104819, 2020.

942 Lopez-Bustins, J.A., Martin-Vide, J., Sanchez-Lorenzo, A.: Iberia winter rainfall
943 trends based upon changes in teleconnection and circulation patterns. Global
944 and Planetary Change 63, 171-176. DOI: 10.1016/j.gloplacha.2007.09.002,
945 2008.

946 Lopez-Bustins, J.A., Martin-Vide, J., Prohom, M., Cordobilla, M.J.: Variabilidad
947 intraanual de la Oscilación del Mediterráneo Occidental (WeMO) y ocurrencia de
948 episodios torrenciales en Cataluña. In: Olcina, J., Rico, A.M., Moltó, E. (eds.),
949 Clima, sociedad, riesgos y ordenación del territorio, pp. 171-182. Alicante
950 (Spain): Asociación Española de Climatología (AEC), 2016.

951 Martin-Vide, J.: Aplicación de la clasificación sinóptica automática de Jenkinson
952 y Collison a días de precipitación torrencial en el este de España. In: Cuadrat,
953 J.M., Vicente-Serrano, S., Saz, M.A. (eds.), La información climática como
954 herramienta de gestión ambiental, pp. 123-127, Zaragoza (Spain): University of
955 Zaragoza, 2002.

956 Martin-Vide, J., Llasat, M.C.: Las precipitaciones torrenciales en Cataluña. Serie
957 Geográfica 9, 17-26, 2000.

958 Martin-Vide, J., Lopez-Bustins, J.A.: The Western Mediterranean Oscillation and
959 rainfall in the Iberian Peninsula. International Journal of Climatology 26, 1455-
960 1475. DOI: 10.1002/joc.1388, 2006.

961 Martin-Vide, J., Raso-Nadal, J.M.: *Atles Climàtic de Catalunya, 1961-1990*. 32
962 pp. Barcelona (Spain): Servei Meteorològic de Catalunya, Departament de Medi
963 Ambient i Habitatge, Generalitat de Catalunya, 2008.

964 Martin-Vide, J.P., Llasat, M.C.: The 1962 flash flood in the Rubí stream
965 (Barcelona, Spain). *Journal of Hydrology* 566, 441-454. DOI:
966 10.1016/j.jhydrol.2018.09.028, 2018.

967 Martin-Vide, J., Sanchez-Lorenzo, A., Lopez-Bustins, J.A., Cordobilla, M.J.,
968 Garcia-Manuel, A., Raso, J.M.: Torrential rainfall in northeast of the Iberian
969 Peninsula: synoptic patterns and WeMO influence. *Advances in Science and*
970 *Research* 2, 99-105. DOI: 10.5194/asr-2-99-2008, 2008.

971 Martina, M.L.V., Todini, E., Libralon, A.: Rainfall thresholds for flood warning
972 systems: a Bayesian decision approach. In: Sorooshian S., Hsu KL., Coppola E.,
973 Tomassetti B., Verdecchia M., Visconti G. (eds.), *Hydrological Modelling and the*
974 *Water Cycle*. Water Science and Technology Library, vol 63, pp. 203-227.
975 Springer, Berlin, Heidelberg (Germany). DOI: 10.1007/978-3-540-77843-1_9,
976 2009.

977 Mathbout, S., Lopez-Bustins, J.A., Royé, D., Martin-Vide, J., Benhamrouche, A.:
978 Spatiotemporal variability of daily precipitation concentration and its relationship
979 to teleconnection patterns over the Mediterranean during 1975-2015.
980 *International Journal of Climatology* 40, 1435-1455. DOI: 10.1002/joc.6278,
981 2020.

982 Merino, M., Fernández-Vaquero, M., López, L., Fernández-González, S.,
983 Hermida, L., Sánchez, J.L., García-Ortega, E., Gascón, E.: Large-scale patterns
984 of daily precipitation extremes on the Iberian Peninsula. *International Journal of*
985 *Climatology* 36, 3873-3891. DOI: 10.1002/joc.4601, 2016.

986 Meseguer-Ruiz, O., Lopez-Bustins, J.A., Arbiol-Roca, L., Martin-Vide, J., Miró, J.,
987 Estrela, M.J.: Episodios de precipitación torrencial en el este y sureste ibéricos y
988 su relación con la variabilidad intraanual de la Oscilación del Mediterráneo
989 Occidental (WeMO) entre 1950 y 2016. In: Montávez-Gómez, J.P., Gómez-
990 Navarro, J.J., López-Romero, J.M., Palacios-Peña, L., Turco, M., Jerez-
991 Rodríguez, S., Lorente, R., Jiménez-Guerrero, P. (eds.), *El Clima: Aire, Agua,*

992 Tierra y Fuego, pp. 53-63. Cartagena (Spain): Asociación Española de
993 Climatología (AEC), 2018.

994 Milosevic, D.D., Savic, S.M., Pantelic, M., Stankov, U., Ziberna, I., Dolinaj, D.,
995 Lescesen, I.: Variability of seasonal and annual precipitation in Slovenia and its
996 correlation with large-scale atmospheric circulation. *Open Geosciences* 8, 593-
997 605. DOI: 10.1515/geo-2016-0041, 2016.

998 Miró, J., Estrela, M.J., Pastor, F., Millán, M.: Análisis comparativo de tendencias
999 en la precipitación, por distintos inputs, entre los dominios hidrológicos del
1000 Segura y del Júcar (1958-2008). *Investigaciones Geográficas* 49, 129-157, 2009.

1001 Miró, J.J., Caselles, V., Estrela, M.J.: Multiple imputation of rainfall missing data
1002 in the Iberian Mediterranean context. *Atmospheric Research* 197, 313-330. DOI:
1003 10.1016/j.atmosres.2017.07.016, 2017.

1004 Nakamura, I., Llasat, M.C.: Policy and systems of flood risk management: a
1005 comparative study between Japan and Spain. *Natural Hazards* 87, 919-943. DOI:
1006 10.1007/s11069-017-2802-x, 2017.

1007 Naranjo-Fernández, N., Guardiola-Albert, C., Aguilera, H., Serrano-Hidalgo, C.,
1008 Rodríguez-Rodríguez, M., Fernández-Ayuso, A., Ruiz-Bermudo, F., Montero-
1009 González, E.: Relevance of spatio-temporal rainfall variability regarding
1010 groundwater management challenges under global change: case study in
1011 Doñana (SW Spain). *Stochastic Environmental Research and Risk Assessment*,
1012 DOI:10.1007/s00477-020-01771-7, 2020.

1013 Norbiato, D., Borga, M., Esposti, S.D., Gaume, e., Anquetin, S.: Flash flood
1014 warning based on rainfall thresholds and soil moisture conditions: An assessment
1015 for gauged and ungauged basins. *Journal of Hydrology* 362, 274-290. DOI:
1016 10.1016/j.jhydrol.2008.08.023, 2008.

1017 Olcina, J., Sauri, D., Hernández, M., Ribas, A.: Flood policy in Spain: a review for
1018 the period 1983-2013. *Disaster Prevention and Management* 25, 41-58. DOI:
1019 10.1108/DPM-05-2015-0108, 2016.

1020 Papalexiou, S.M., Montanari, A.: Global and regional increase of precipitation
1021 extremes under global warming. *Water Resources Research* 55, 4901-4914.
1022 DOI: 10.1029/2018WR024067, 2019.

1023 Pastor, F., Valiente, J. A., Estrela, M. J.: Sea surface temperature and torrential
1024 rains in the Valencia region: modelling the role of recharge areas. *Natural*
1025 *Hazards and Earth System Sciences* 15, 1677-1693, 2015.

1026 Pastor, F., Valiente, J.A., Palau, J.L.: Sea Surface Temperature in the
1027 Mediterranean: Trends and Spatial Patterns (1982–2016). *Pure and Applied*
1028 *Geophysics* 175, 4017–4029. DOI:10.1007/s00024-017-1739-z, 2018.

1029 Peña, J.C., Aran, M., Pérez-Zanón, N., Casas-Castillo, M.C., Rodríguez-Solà, R.,
1030 Redaño, A.: Análisis de las situaciones sinópticas correspondientes a episodios
1031 de lluvia severa en Barcelona. In: Libro de Resúmenes de la XXXV Reunión
1032 Bienal de la Real Sociedad Española de Física, pp. 450-451. Gijón (Spain): Real
1033 Sociedad Española de Física (RSEF), 2015.

1034 Peñarrocha, D., Estrela, M.J., Millán, M.: Classification of daily rainfall patterns in
1035 a Mediterranean area with extreme intensity levels: the Valencia region.
1036 *International Journal of Climatology* 22, 677-695. DOI: 10.1002/joc.747, 2002.

1037 Pérez-Cueva, A.J.: Atlas Climàtic de la Comunitat Valenciana (1961-1990), 205
1038 pp. Valencia (Spain): Generalitat Valenciana, 1994.

1039 Pérez-Zanón, N., Casas-Castillo, M.C., Peña, J.C., Aran, M., Rodríguez-Solà, R.,
1040 Redaño, A., Solé, G.: Analysis of synoptic patterns in relationship with severe
1041 rainfall events in the Ebre Observatory (Catalonia). *Acta Geophysica* 66, 405-
1042 414. DOI: 10.1007/s11600-018-0126-1, 2018.

1043 Raicich, F., Colucci, R.R.: A near-surface sea temperature time series from
1044 Trieste, northern Adriatic Sea (1899-2015). *Earth System Science Data* 11, 2,
1045 761-768, 2019.

1046 Riesco, J., Alcover, V.: Predicción de precipitaciones intensas de origen marítimo
1047 mediterráneo en la Comunidad Valenciana y la Región de Murcia. 124 pp. Madrid
1048 (Spain): Centro de Publicaciones, Secretaría General Técnica, Ministerio de
1049 Medio Ambiente, 2003.

1050 Rigo, T., Llasat, M.C.: Features of convective systems in the NW of the
1051 Mediterranean Sea. Proceedings of the 5th EGU Plinius Conference on
1052 Mediterranean Storms 1-2 October 2003, Ajaccio, France. European
1053 Geosciences Union, pp. 73-79, 2003.

1054 Ríos-Cornejo, D., Penas, A., Álvarez-Esteban, R., del Río, S.: Links between
1055 teleconnection patterns and precipitation in Spain. *Atmospheric Research* 156,
1056 14-28. DOI: 10.1016/j.atmosres.2014.12.012, 2015a.

1057 Ríos-Cornejo, D., Penas, A., Álvarez-Esteban, R., del Río, S.: Links between
1058 teleconnection patterns and mean temperature in Spain. *Theoretical and Applied*
1059 *Climatology* 122, 1-18. DOI: 10.1007/s00704-014-1256-2, 2015b.

1060 Rodó, X., Baert, E., Comin, F.A.: Variations in seasonal rainfall in Southern
1061 Europe during the present century: relationships with the North Atlantic
1062 Oscillation and the El Niño-Southern Oscillation. *Climate Dynamics* 13, 275-284,
1063 1997.

1064 Rodríguez-Puebla, C., Encinas, A.H., Sáenz, J.: Winter precipitation over the
1065 Iberian Peninsula and its relationship to circulation indices. *Hydrology and Earth*
1066 *System Sciences* 5, 233-244, 2001.

1067 Romero, R., Sumner, G., Ramis, C., Genovés, A.: A classification of the
1068 atmospheric circulation patterns producing significant daily rainfall in the Spanish
1069 Mediterranean area. *International Journal of Climatology* 19, 765-789, 1999.

1070 Salat, J., Pascual, J., Flexas, M., Chin, T.M., Vazquez-Cuervo, J.: Forty-five
1071 years of oceanographic and meteorological observations at a coastal station in
1072 the NW Mediterranean: a ground truth for satellite observations. *Ocean Dynamics*
1073 69, 1067–1084, 2019.

1074 Sánchez-García, C., Schulte, L., Carvalho, F., Peña, J.C.: A 500-year flood
1075 history of the arid environments of southeastern Spain. The case of the
1076 Almanzora River. *Global and Planetary Change* 181, DOI:
1077 10.1016/j.gloplacha.2019.102987, 2019.

1078 SMC-Servei Meteorològic de Catalunya: Yearly Bulletin of Climate Indicators,
1079 2016. Technical report. Meteorological Service of Catalonia, Department of
1080 Territory and Sustainability, Government of Catalonia, Barcelona, 88 pp.
1081 Available at: [https://static-m.meteo.cat/wordpressweb/wp-](https://static-m.meteo.cat/wordpressweb/wp-content/uploads/2017/05/29072030/00_BAIC-2016_TOT.pdf)
1082 [content/uploads/2017/05/29072030/00_BAIC-2016_TOT.pdf](https://static-m.meteo.cat/wordpressweb/wp-content/uploads/2017/05/29072030/00_BAIC-2016_TOT.pdf). Climate monthly
1083 series available at: [https://www.meteo.cat/wpweb/climatologia/serveis-i-dades-](https://www.meteo.cat/wpweb/climatologia/serveis-i-dades-climatiques/series-climatiques-historiques/)
1084 [climatiques/series-climatiques-historiques/](https://www.meteo.cat/wpweb/climatologia/serveis-i-dades-climatiques/series-climatiques-historiques/), 2017.

- 1085 Sneyers, R.: On the use of statistical analysis for the objective determination of
1086 climate change. *Meteorologische Zeitschrift* 1, 247–256, 1992.
- 1087 Soler, X., Martin-Vide, J.: Los calendarios climáticos. Una propuesta
1088 metodológica. In: Guijarro, J.A., Grimalt, M., Laita, M., Alonso, S. (eds.), *El Agua
1089 y el Clima*, pp. 577-586. Mallorca (Spain): Asociación Española de Climatología,
1090 2002.
- 1091 Sparnocchia, S., Schiano, M.E., Picco, P., Bozzano, R., Cappelletti, A.: The
1092 anomalous warming of summer 2003 in the surface layer of the Central Ligurian
1093 Sea (Western Mediterranean). *Annales Geophysicae* 24, 2, 443-452, 2006.
- 1094 Trigo, R.M., Pozo-Vázquez, D., Osborn, T.J., Castro-Díez, Y., Gámiz-Fortis, S.,
1095 Esteban-Parra, M.J.: North Atlantic Oscillation influence on precipitation, river
1096 flow and water resources in the Iberian Peninsula. *International Journal of
1097 Climatology* 24, 925-944. DOI: 10.1002/joc.1048, 2004.
- 1098 Vicente-Serrano, S.M., Beguería, S., López-Moreno, J.I., El Kenawy, A.M.,
1099 Angulo-Martínez, M.: Daily atmospheric circulation events and extreme
1100 precipitation risk in northeast Spain: Role of the North Atlantic Oscillation, the
1101 Western Mediterranean Oscillation, and the Mediterranean Oscillation. *Journal of
1102 Geophysical Research* 114, D08106. DOI: 10.1029/2008JD011492, 2009.
- 1103 Vigneau, J.-P.: 1986 dans les Pyrénées Orientales: deux perturbations
1104 méditerranéennes aux effets remarquables. *Revue Géographique des Pyrénées
1105 et du Sud-Ouest* 58, 23-54. DOI:10.3406/rgpso.1987.4969, 1987.
- 1106 Wergen, D., Volovik, D., Redner, S., Krug, J.: Rounding Effects in Record
1107 Statistics. *Physical Review Letters* 109(16): 164102. DOI:
1108 10.1103/PhysRevLett.109.164102, 2012.